Tutor/s

Dr. Jordi Hug Badia i Córcoles
Chemical Engineering & Analytical Chemistry Dept.

Dra. Eliana Ramírez Rangel
Chemical Engineering & Analytical Chemistry Dept.

Grau en Enginyeria Química

Treball Final de Grau

Start-up of the experimental setup for the hydrogenation reaction of levulinic acid to γ-Valerolactone over a Pd-doped ion-exchange resin

Marta Miras Gil

January 2021

UNIVERSITAT DE BARCELONA

ACKNOWLEDGMENTS

I would like to thank all those who have collaborated in some way in the development of this project.

First of all, I wish to thank my teachers of this project, Eliana Ramírez Rangel and Jordi Hug Badia i Córcoles for their dedication and attention for at any time that I have needed them, and for trusting me since the beginning of this important project. Thank you for placing your trust in my ability.

Secondly, I want to thank my friends, both the new and the old ones, for accompanying me in the development of this project.

I also wish to express my gratitude to my family for their efforts and support during this unprecedented year, and finally thanks to all the teachers with whom I have shared class during the last four years.

CONTENTS

SUMMARY

The conversion of organic matter into value-added products is a field of research that has gained importance in recent years, due to the need to reduce the use of fossil fuels.

Lignocellulose is the most abundant biological renewable resource on Earth. The Biofine Process can transform carbohydrate feedstock from lignocellulose into platform chemical products such as levulinic acid, furfural and formic acid. Gamma-valerolactone, a fuel additive and precursor of many value-added compounds, can be obtained by catalytic hydrogenation of levulinic acid.

The start-up of the installation available in the laboratory has been made in order to be able to perform the hydrogenation reaction of levulinic acid catalyzed by a bifunctional cation exchange resin doped with palladium. The analysis system has been developed and calibrated, and Standard Operating Procedures have been developed to carry out the studied reaction.

Keywords: Gamma-valerolactone, Amberlyst CH28, hydrogenation, levulinic acid, Standard Operating Procedures, lignocellulose, biomass.

RESUMEN

La transformación de materia orgánica en productos de valor agregado es un campo de investigación que ha cobrado importancia en los últimos años, debido a la necesidad de reducir el uso de combustibles fósiles.

La lignocelulosa es el recurso biológico renovable más abundante en la Tierra. El proceso Biofine puede transformar la materia prima de carbohidratos de la lignocelulosa en moléculas plataforma como el ácido levulínico, el furfural y el ácido fórmico. La gamma-valerolactona, un aditivo de combustible y precursor de muchos compuestos de valor agregado, se puede obtener mediante hidrogenación catalítica de ácido levulínico.

La puesta en marcha de la instalación disponible en el laboratorio se ha realizado para poder realizar la reacción de hidrogenación del ácido levulínico catalizada por una resina de intercambio catiónico bifuncional dopada con paladio. Se ha desarrollado y calibrado el sistema de análisis y se han desarrollado los Protocolos Normalizados de Trabajo para llevar a cabo la reacción estudiada.

Palabras clave: Gamma-valerolactona, Amberlyst CH28, hidrogenación, ácido levulínico, Protocolos Normalizados de Trabajo, lignocelulosa, biomasa

RESUM

La transformació de matèria orgànica en productes de valor afegit és una àrea de recerca que ha cobrat importància en els últims anys a causa de la necessitat de reduir l'ús de combustibles fòssils.

La lignocelulosa és el recurs biològic renovable més abundant a la Terra. El procés Biofine pot transformar la matèria prima de carbohidrats de la lignocelulosa en molècules plataforma com l'àcid levulínic, el furfural i l'àcid fòrmic. La gamma-valerolactona, un additiu dels combustibles i precursor de molts compostos de valor afegit, es pot obtenir mitjançant la hidrogenació catalítica d'àcid levulínic.

La posada en marxa de la instal·lació disponible al laboratori s'ha realitzat per tal de poder dur a terme la reacció d'hidrogenació de l'àcid levulínic catalitzada per una resina d'intercanvi catiònic bifuncional dopada amb pal·ladi. S'ha desenvolupat i calibrat el sistema d'anàlisi i s'han desenvolupat els Protocols Normalitzats de Treball per dur a terme la reacció estudiada.

Paraules clau: Gamma-valerolactona, Amberlyst CH28, hidrogenació, àcid levulínic, Protocols Normalitzats de Treball, lignocelulosa, biomassa.

1. INTRODUCTION

Biomass is the term used to refer to all organic matter that can be obtained from photosynthesis and used as a source of energy. The biomass energy can come from different origins, such as plant or animals, and it can be obtained naturally or may need to have some chemical process applied to obtain it. As biomass is a renewable and not limited energy source, it has gained importance lately due to limited energy sources problem, such as fossil fuels.

Biomass is therefore a suitable raw material to produce biofuels as a source of energy. These can be classified into first, second, third and fourth generation biofuels depending on the raw materials used [1].

- **First generation biofuels**: Fuels made from food crops grown on arable lands.
- **Second generation biofuels**: Fuels made from lignocellulosic biomass or agricultural residues.
- **Third generation biofuels**: Fuels made from algae sources.
- **Fourth generation biofuels**: Solar biofuels by synthetic biology technologies.

As it has been mentioned, second generation biofuels are those that have lignocellulose as their raw material, making these ones an interesting alternative to produce biofuels. These are a better option than first generation biofuels since lignocellulosic raw materials do not compete with food crops and are also more competitively priced than conventional agricultural raw materials.

On the other hand, third and fourth generation biofuels are not competitive with first and second generation ones due to the fact that they have not yet developed as much as the other ones [1].

As shown in Figure 1, since the early 21st century, biofuels production has increased more than 7 times [2]. In 2019, Spain biodiesel consumption was about 77 thousand metric tons, and in 2010 its consumption reached its highest peak, with 344.56 thousand metric tons consumed [3].

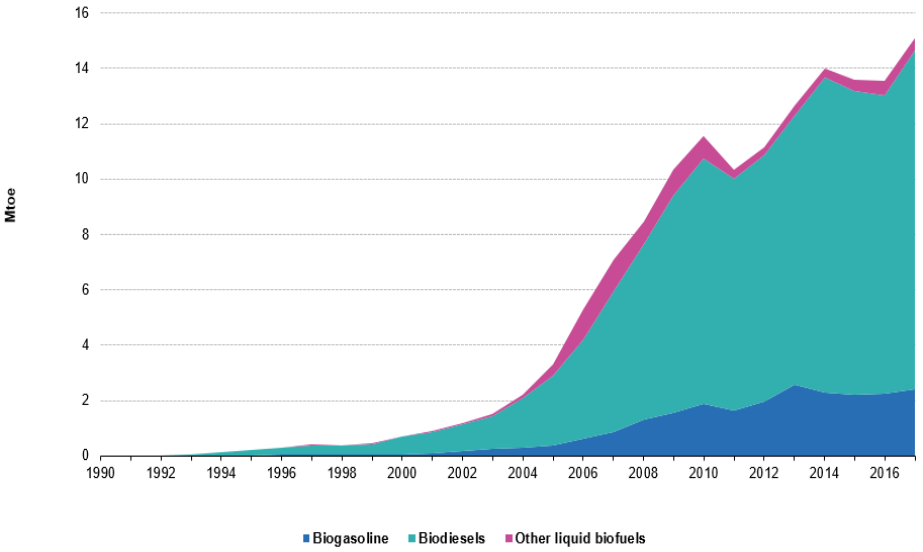

Figure 1: Production of liquid biofuels in EU [2]

Even though lignocellulosic biomass is a very abundant raw material for biofuels production, supply-chain need to produce second generation biofuels presents dire difficulties since using only agricultural and wood residues are not enough to cover current demand [4]. One alternative path that has been developed lately is to integrate second generation biofuels production into existing manufacturing processes with biomass residues such as paper production.

The main problem with these biofuels is the difficulty in some steps of production such as the enzymatic decomposition of sugars or gasification. These complications may be due to genetic and environmental influences such as new crosslinking bonds in the lignocellulose structure.

The transformation of lignocellulose into biofuels or fuels additives is a necessary field of investigation for the following years. From lignocellulose biomass levulinic acid can be obtained and by hydrogenation of levulinic acid, one of these widely used additives, gamma-valerolactone can be produced. Gamma-valerolactone is a forerunner of many value-added products for

refineries. Therefore, both the study and the optimization of the gamma-valerolactone production process may be a future interesting field of research.

2. OBJECTIVES

The main purpose of this project is to contribute to the study of the hydrogenation reaction of levulinic acid catalyzed by a bifunctional cation exchange resin doped with palladium.

The specific goals for the present project are the following:

- To conduct a bibliographical search aimed at describing previous experiences regarding the hydrogenation reaction of levulinic acid.
- To conduct a bibliographical study focused on the description of bifunctional ion exchange resins and activation protocols found in the open literature for the ion-exchange resin used as the catalyst in the present project, Amberlyst CH28.
- To perform an adaptation of an existing experimental setup in the laboratory in order to carry out its subsequent start-up.
- To prepare all necessary Standard Operating Procedures (SOPs) aimed at development for the reaction studied in the facility available in the laboratory.

3. FRAME OF THE STUDY

3.1 LIGNOCELLULOSE

Lignocellulosic biomass is the most abundant biological renewable resource on Earth, its global structure is globally composed of three polymers bonded together, namely: cellulose, hemicellulose and lignin (see Figure 2).

Chemical composition of biomass depends basically on its source but generally consists of 40-80% of cellulose, 10-40% of hemicellulose and lignin between 5 and 25%, with the rest of its constituents being minority compounds [5].

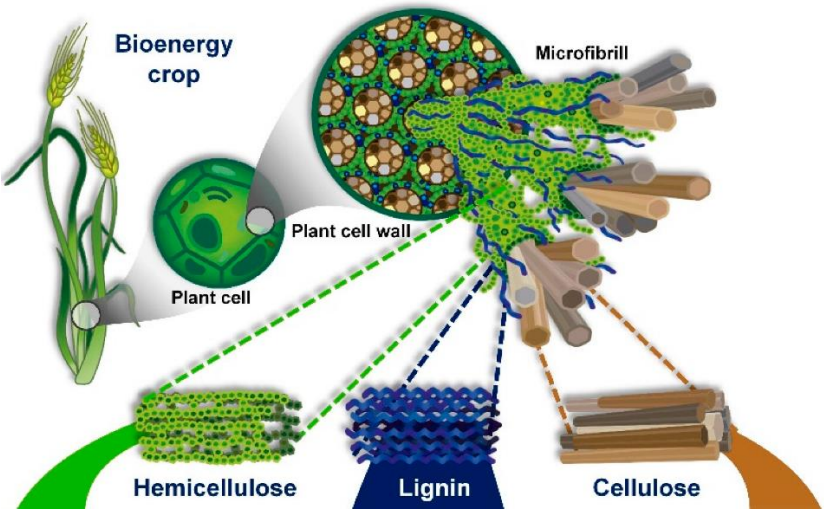

Figure 2: Structure of lignocellulosic biomass [5]

- **Cellulose**: This is an organic compound that consists of a vast linear chain of glucose units, its chemical formula is $(C_6H_{10}O_5)_n$ where n represents the number of glucose units. It is the most abundant organic polymer on Earth, it is also insoluble in water and almost all organic solvents, chiral and biodegradable.

- **Hemicellulose**: This is a polysaccharide composed of more than one type of monosaccharide. Its structure is short, highly ramified, amorphous and has little strength. It can be hydrolyzed in either acid or basic medium.
- **Lignin**: This is an aromatic polymer and its chemical composition varies between species. It is insoluble in water, has an amorphous and tridimensional structure, is highly ramified and has a high molecular weight.
- **Minority compounds**: These are generally classified into ashes, extractable compounds and proteins. They have a lower molecular weight compared to the other three main compounds.

3.2 THE BIOFINE PROCESS

The Biofine Process is one of the most advanced and commercially viable lignocellulosic-fractionating technologies currently available [6]. It can transform carbohydrate feedstock into platform chemical products such as levulinic acid (LA), furfural and formic acid (FA). The process involves the hydrolysis of polysaccharides to their monomeric constituents, and these are then, in turn, continuously converted to valuable platform chemicals [6].

The Biofine Process (see Figure 3) uses diluted sulfuric acid as a catalyst and produces levulinic acid and furfural as its final products. This diluted acid converts the five and six carbon sugars from lignocellulose into furfural and Hydroxymethylfurfural (HMF) which is later converted into levulinic acid after longer residence times.

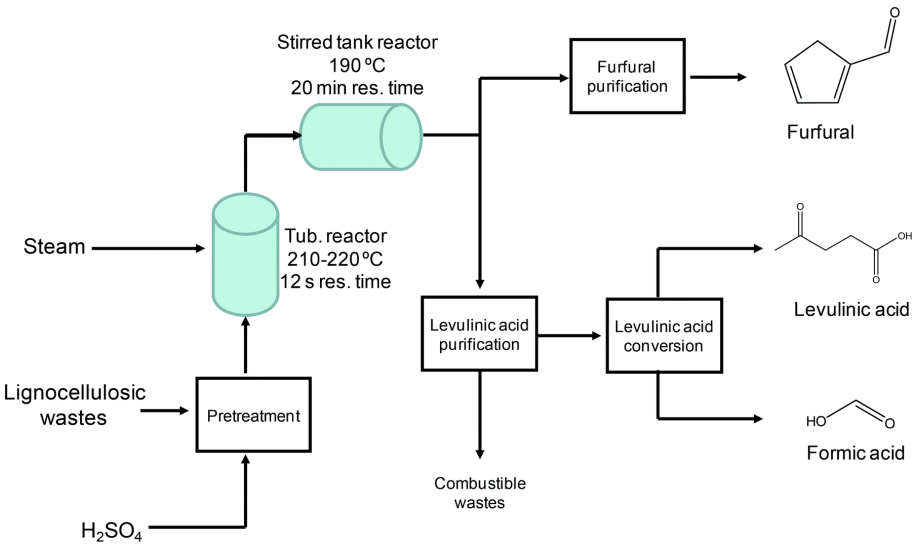

Figure 3: Flow chart of Biofine Process [48]

This process consists of two distinct acid-catalyzed stages that operate to give optimal yields (between 70 and 80%) with minimum degradation of products.

In the first reactor, an acid hydrolysis of the carbohydrate polysaccharides is made. This step has a very low residence time, which involves small diameter reactors. This reactor operates at 210-220 °C, a pressure of 25 bar and a 12 second residence time. This reactor is considerably larger than the first one and, therefore, its residence times are higher. The second reactor operates at less severe conditions such as 190-200 °C, a pressure of 14 bar and a residence time of approximately 20 minutes. Yields for the Biofine Process depend on reaction conditions and composition of the raw material used [6].

Apart from cellulose and LA, there are others intermediates that are not useful for this reaction and decrease the global yield, some authors have estimated that there are over 100 of these. These intermediates usually react to form some tar which incorporates many insoluble residues that are later difficult to separate from the products.

Among all platform chemicals produced, LA is well known as a chemical bridge between raw biomass and value-added products.

3.3 LEVULINIC ACID

Levulinic acid is an organic compound with the formula $C_5H_8O_3$ (see Figure 4). It is a straight-chain saturated fatty acid and has an oxopentanoic acid in its fourth position. LA is also known as a keto acid, which means that it has two highly reactive functional groups, a carboxylic acid and a ketone.

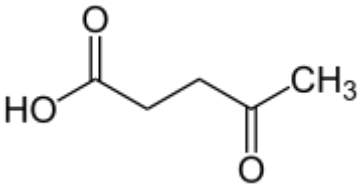

Figure 4: Levulinic Acid formula

Its melting point is between 33 and 35 °C which means that at room temperature it has a white crystalline solid appearance. It is soluble in water (675 g/L at 25 °C) and in most polar organic solvents but is insoluble in aliphatic hydrocarbons [35, 54].

In 2004 LA was one of the 12 most valuable platform compounds identified by the US Department of Energy [47]. It is highly used as a precursor for many fuel additives such as 2-methyltetrahydrofuran (MTHF), ethyl levulinate, angelica lactone (AL) and gamma-valerolactone (GVL).

3.4 GAMMA-VALEROLACTONE

Gamma-valerolactone (GVL) is an organic compound with the formula $C_5H_8O_2$ (see Figure 5). It is a cyclic ester, a chiral molecule and has one double bond. At room temperature, it is a colorless liquid with a density similar to water and it is soluble in both water and organic solvents. Due to its herbal odor, it is commonly used in the perfume industry and its possible leaks are easy to detect. GVL has low toxicity (LD_{50}= 8800 mg/kg) [8, 11, 12].

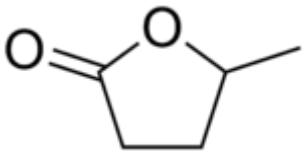

Figure 5: GVL formula

The main risk of GVL is flammability; however, its low volatility makes the flammability risk at normal conditions actually low. It has a 96 °C melting point that minimizes the ignition hazard. On the other hand, its vapor pressure is low at high temperatures, about 3.5 kPa around 80 °C [7].

As can be seen in Figure 6 [59] there is a wide variety of possible routes to convert GVL into those value-added compounds mentioned before.

Routes shown into both orange colored bubbles are the ones related to fuels and its additives.

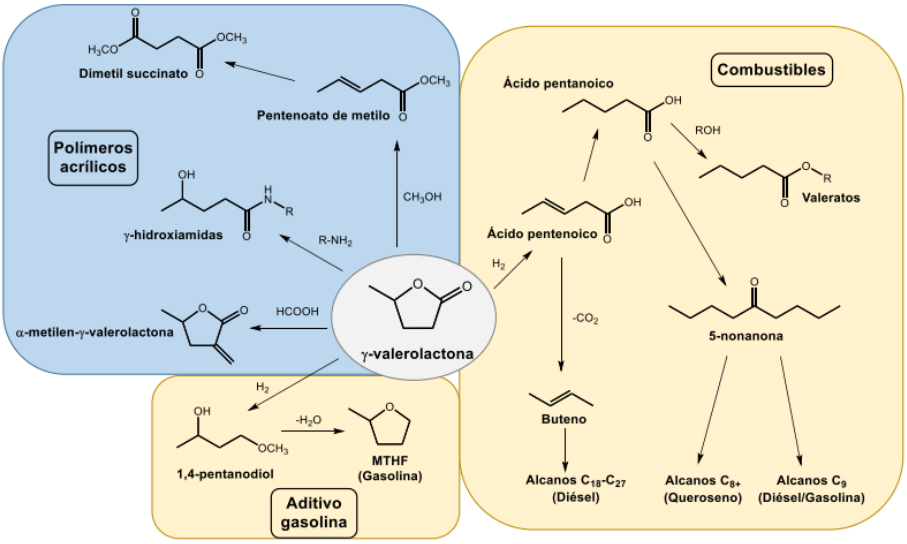

Figure 6: Possible routes to convert GVL into value-added compounds [59]

The most important use of GVL nowadays is as diesel and gasoline additive because it improves combustion due to its low vapor pressure [12]. Its production cost is still very high but it is expected to decrease as the production of LA increases [11]. Currently, new technologies are being researched and developed (see blue bubble in Figure 6) which use GVL as a precursor of high chemical value-added compounds such as ionic liquids and polymers.

Table 1 shows the main physical properties of GVL in comparison to ethanol (EtOH) [15].

Table 1: Properties of GVL in comparison to ethanol fuel

Properties	GVL	EtOH
M [g/mol]	100.12	46.07
Carbon [wt. %]	60	52.2
Boiling point [°C]	207	78
Melting point [°C]	-31	-114
Flash point [°C]	96.1	13
Density [g/mL]	1.049	0.789
Solubility in water [mg/mL]	≥100	Miscible
Octane number	95.4	108.6
Cetane number	Not specified	5
ΔHvap [kJ/mol]	-54.8	42.59
ΔcH° liquid [kJ/mol]	-1367.6	-2649.6

Comparative evaluation of GVL and ethanol as fuel additives, performed on a mixture of 10 % vol. GVL or ethanol and 90 % vol. 95-octane gasoline, shows very similar properties. GVL is a good substitutive of EtOH in fuels, since GVL does not form an azeotrope with water. It can also be later readily removed by distillation, resulting in a less energy demanding process for the production of GVL than that of absolute ethanol [13].

In comparison to fossil fuels, GVL has a lower energy density and higher water solubility, which limits its direct application in transportation fuel production [7]. On the other hand, CO emissions from a GVL-blended fuel are significantly reduced in comparison with a 100% fossil diesel [14].

4. GVL PRODUCTION

The two most known routes to produce GVL from LA are shown in Figure 7. The first route is the hydrogenation of LA to 4-hydroxypentanoic acid. 4-Hydroxypentanoic acid is an unstable intermediate product that closes its structure to create a ring by intramolecular esterification, losing a water molecule and then producing GVL. The second route starts by losing one water molecule in order to close the LA chain, creating a ring. Then, by catalyzed hydrogenation, a double bond is broken and GVL is produced [7,8, 11].

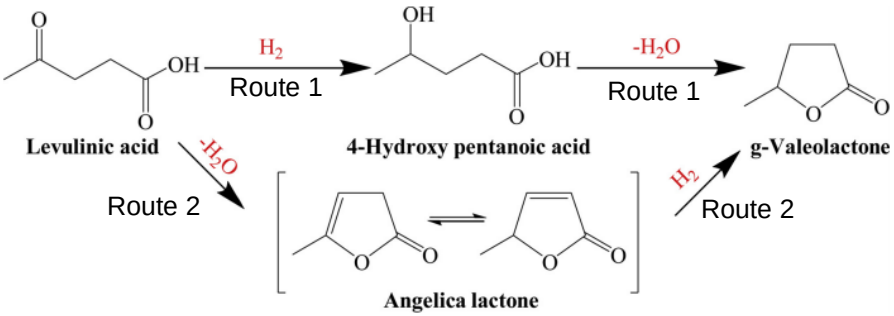

Figure 7: Reaction paths of LA to GVL [16]

Hydrogenation with molecular hydrogen is the most common way to reduce organic unsaturated acids such as LA. This process normally need high pressures and noble metal catalysts, either in heterogenous and homogeneous transformations [8, 9].

Alternatively, as theoretically, the hydrolysis of cellulose to LA is accompanied by the equimolar formation of formic acid; FA may be used as the molecule which releases hydrogen upon breakage [8, 10, 16].

GVL production form LA following the Route 1 is the reaction selected to be studied in the present work.

Thus, the overall process to obtain GVL from LA involves two subsequent steps of hydrogenation and esterification. The former requires presence of a metal catalyst and the latter acid catalyst.

4.1 GVL PRODUCTION VIA HOMOGENEOUS CATALYSIS

It has been demonstrated that the use of homogeneous catalysts in the studied reaction can provide high yields of GVL under mild reaction conditions [17-20].

The fact that homogeneous catalysts can act as a single active site is a great advantage and makes them become more active and selective. As can be seen in Table 2 [15], homogeneous catalysis reactions have been reported with good conversions of LA and, mostly, with high selectivity to GVL.

Recently, new metal catalyst technologies such as Iridium based complex catalyst and different water-soluble ligands in Ru-based catalysts, have been screened to be a viable resource in GVL production [17-20].

Table 2: Hydrogenation of LA using homogeneous catalysts

Substrate	Catalyst	T [°C]	Reaction time [h]	Y_{GVL} [%]
LA	$Ru(acac)_3$+TPPTS	140	12	95
LA	$Ru(acac)_3$+PBu_3	200	6	37
LA	$Ru(acac)_3$+$PnOct_3$+NH_4PF_6	160	18	>99
LA	$RuCl_2(PPh_3)$	180	24	99
LA	$RuH_2(PPh_3)_4$	180	24	58
LA	$RuCl_3 \cdot H_2O/PPh_3$	150	12	93

4.2 GVL PRODUCTION VIA HETEROGENEOUS CATALYSIS

Due to the necessity to fit hydrogenation conditions and, simultaneously, the acid catalysis, the metal is usually combined with various carriers to satisfy both necessities.

A heterogeneous catalyst facilitates sufficient contact of the substrate with the catalyst to achieve a higher catalytic efficiency. The advantage of heterogeneous catalysis often involves easy later separation, efficient recycling, minimization of metal leaching and a higher process control.

Heterogeneous non-noble metal catalysts have gained importance in recent years due to the cost difference compared to noble metal catalysts. The non-noble metal Nickel (Ni) has attracted extensive attention due to its high catalytic activity. It has also been noted that the simultaneous use of Copper (Cu) and other metals such as Zirconium (Zr) and Aluminum (Al) exhibit excellent catalytic properties too. Multi-metal combination has been studied lately and it seems to be a feasible method in the future [15, 16].

On the other hand, noble-metal catalysts are the most used heterogeneous catalyst in hydrogenation due to the large surface area and the high synergic effect between metal nanoparticle and support [15]. The most commonly used supported noble-metals are Ruthenium (Ru), Rhodium (Rh), Palladium (Pd) and Platinum (Pt). Supported Gold (Au) support is the least used catalyst since it is the most expensive and the one where fewer industrial applications have been found.

Table 3 summarizes the experiments performed to produce GVL using noble-metal catalysts [15, 21-26].

Table 3: Production of GVL using noble-metal catalysts

Substrate	Catalyst	T [°C]	Reaction time [h]	Y_{GVL} [%]
LA	Ru/C	150	4	97
LA	Ru/SiO_2	200	Not specified	>99
LA	$Ru\text{-}P/SiO_2$	150	6	30
LA	Ru/TiO_2	150	1	63
LA	Pd/Al_2O_3	220	12	29
LA	5% Ru/Al_2O_3	201	Not specified	75.3
LA	5% Rh/C	141	Not specified	98.9
LA	Au/TiO_2	150	6	55
LA	5% Au/ZrO_2	140	5	66
LA	5% Ru/Hydroxyapatite	70	4	99

The studied reaction mechanism using noble-metal catalysts (see Figure 7 from Section 4) starts by the hydrogenation reaction of molecular hydrogen and liquid LA on the metal support. Hydrogen is absorbed in the noble-metal surface to form a bond and LA is then is absorbed too

by the combination of the noble-metal with carbonylic C and O atoms. The result is the formation of the intermediate product 4-hydroxipentanoic acid, which then forms GVL by dehydrogenation.

To perform this one-pot synthesis, both steps may be catalyzed and, for that reason, bifunctional catalysts are more commonly used. In this metal–acid bifunctional catalyst system, it is thought that the acid function plays a role in the dehydration reaction and the metal catalysis hydrogenation reaction. In the present project, a bifunctional Pd and cation-exchange resin has been used as catalyst in order to fulfill both acid and metal catalytic requirements of the studied reaction.

5. BIFUNCTIONAL ION EXCHANGE RESINS

Bifunctional catalysts, like the one used in the present work, have two types of active sites in their structure which enable different reactions to occur subsequently, and might present different activities for each one.

Multiple reactions involving acid catalysis followed by hydrogenation or dehydrogenation and vice versa are very common in many industrial processes. If the conditions for both reactions are overlapping, they can advantageously be performed in a single step with a bifunctional catalyst [27].

Resins catalysts can be obtained by the attachment of metal species to polymerized materials, such as epoxy or divinylbenzene, via several immobilization techniques. The characteristics of the resin support will be determined by the type of polymer that constitutes it and by its structure. Addition polymers have been used, such as polystyrene and acrylic polymers; and also, condensation polymers, such as phenolic or epoxy-amines ones.

Styrene-divinylbenzene matrix sulfonic resins are the most widely used [58]. These resins have a second production process where the polymerized matrix is sulfonated by an electrophilic aromatic substitution reaction.

Resins doped with Molybdenum, Palladium, or Rhodium species were commonly prepared and used as recyclable catalysts for epoxidation, carbon–carbon coupling, hydrogenation, and hydroformylation reactions [57].

Ion exchange resins are organic materials, insoluble in water and solids, presented in spherical form or pearls with an effective size between 0.3 and 1.2 mm, there are some resins in powder form too. As mentioned before, resins are composed by a polymeric matrix to which a large number of polar radicals, acids or bases, have been attached. When a solvent goes through the resin, the resin takes ions from the solvent and exchanges them with those radicals impregnated in the resin. Supported metal catalyst requires that the supported metal should have good dispersity and stability on its support.

Ion exchange resins can usually be regenerated, which means that when the ion exchange capacity has been exhausted, a regenerating solution can be used to fully recover the resin original exchange capacity. This regeneration can be achieved by passing the solution with the original ion through the resin, which binds to the radicals in the resin and displaces the captured ions during normal operation. Resins used in catalysis are almost never regenerated since using new ones is cheaper for the global process. This regeneration process is common in resins that are used for water ultra-purification [55].

The two main types of ion exchanging resins, according to their functional groups, are cation exchange and anion exchange resins. Cation exchange resins interchange Hydrogen H^+ ions or other ions as an exchange for cations present in the solvent. Anion exchange resins release hydroxyl OH^- ions or other negatively charged ions in exchange for the ions present in the solvent [28].

In addition, according to their structure, two large types of commercial resins can be distinguished: microporous and macroporous resins. Microporous resins can also be named as gel-type resins. These resins are produced by the polymerization of divinylbenzene and styrene. The ions to be exchanged diffuse through the gel structure to interact with exchange sites. Gel-type resins are thermally stable and exhibit high exchange capacity. On the other hand, macroporous resins have an area/volume ratio bigger than those of the gel-type; as they offer greater stability with thermal and mechanical perturbations, they are commonly used as catalysts. Compared to gel-type resins, macroporous ones have a lower ion exchange capacity, however, this is compensated by their longer useful life [55].

The main difference between microporous and macroporous resins is that the first ones only have that gel phase and the second ones also have stable macropores in its structure. The gel phase is the part of the structure of the resin that is altered depending on the polarity of the medium in which it is found. Then, the swelling suffered by the microporous resins is much more important, they can triple or quadruple in size, than the macroporous ones.

The use of resins as a catalyst compared to conventional catalysts, means an increase of the process rate and the formation of secondary reactions is avoided. Resins can be easily separated from the rest of the reaction reactants, they retain their activity for a long time and can be regenerated, a fact that allows work in continuous flow reactors and long life systems [58].

In this project, a bifunctional Pd-doped cation exchange commercial resin commercially known as Amberlyst CH28 has been used in order to perform the studied reaction. The resin used in this project is a macroporous sulphonated resin. No studies have been reported to use this catalyst for the hydrogenation of LA, but as it is one of the most common commercial bifunctional resins available in the market nowadays, its use in this reaction is an important field for future investigation.

5.1 AMBERLYST CH28

As mentioned before, the Amberlyst CH28 catalyst is a metal doped bifunctional cation exchange commercial resin. It is doped with Palladium and widely used in hydrogenation reactions, as the palladium usually prevents the formation of higher condensation. It is supplied by DuPont, has a bead form and presents a stable macroporous structure.

Its properties are specified in Table 4 [33].

Table 4: Amberlyst CH28 properties

Palladium load	0.7 % minimum in dry basis
Matrix	Styrene DVB polymer
Concentration of acid sites [eq/L]	≥ 1.6
Surface area [m^2/g]	36
Average pore diameter [Å]	260
Water retention capacity	52 – 58 %
Particle diameter [µm]	850 – 1050
Maximum operating temperature [°C]	130
LHSV operating range [h^{-1}]	0.5 – 5
Density [g/L]	790

With regard to catalyst characterization, Table 5 summarizes and compares the most important resin characteristics in both wet and dry conditions, as determined by Institute of Chemical Process Fundamentals (ICPF) in Prague.

Table 5: Amberlyst CH28 characterization data

	Wet conditions	Dry conditions
Pore diameter [nm]	8.91	8.71
Pore volume [cm^3/g]	0.293	0.295
Specific surface [m^2/g]	133.4	137.2
True swollen polymer volume [cm^3/g]	1.147	1.128

From the properties displayed in Table 5, it can be concluded that in wet conditions the resin expands, as its pores are bigger than in dry conditions, this facilitates the access of the reactants to the active centers of the catalyst.

5.2 ACTIVATION PROTOCOLS FOR AMBERLYST CH28

Metal catalysts need a previous treatment before being used as a catalyst in any reaction, this treatment is known as activation. Activation of a metal catalyst consists of reduction of the metal oxidation state since it is usually impregnated on the catalyst support in its oxidized form. In particular, Pd-doped catalysts are reduced with hydrogen, from Pd^{+2} to Pd^0. There are several scientific papers where the different activation methods for this resin are explained.

For instance, Nicol and Du Toit [29], who studied the synthesis of methyl isobutyl ketone (MIBK) from acetone, performed a previous Palladium reduction before the reaction. They allowed an acetone and hydrogen flow (3.3 mL/min and 330 mL/min respectively) through a fixed bed reactor. After 4 hours at 30 bar, no significant changes in the outlet concentration were observed, so it was deduced that no additional reduction of palladium took place. They also checked the catalyst deactivation using the same catalyst for more than one run. They concluded that the catalyst bed had a good stability and an acceptable repeatability.

For the same acetone hydrogenation reaction, Talwalkar and Mahajani [27] performed an experiment in an autoclave stirred-tank reactor, but they did not carry out a previous activation of the catalyst. A reactor volume of 80 mL was filled with the desired quantities of the catalyst and 100 g of acetone each time. The reaction mixture was heated up and the stirring speed was activated. When the reaction reached 2.5 hours approximately, it was considered that the system reached the steady state.

Prinsloo et al. [30] also studied the production of MIBK from acetone using Amberlyst CH28 as a catalyst. They did not activate the catalyst before performing the reaction; in fact, they preheated an acetone and hydrogen mixture and fed it directly to a trickle-bed reactor.

However, for the same reaction mentioned, Trejo et al. [31] performed a previous activation step of the catalyst. It was performed with hydrogen at 20 bar and 100 °C for 24 hours.

Käldström et al. [32] studied the carbon chain length increase reactions of platform molecules derived from C5 and C6 sugars. They used Amberlyst CH28 as the catalyst in the aldol condensation of 2-pentanone acid without previous catalyst activation, 0.1 g of catalyst were used for each feed gram under 6 L/h of hydrogen flow. They specified that the resin catalyst was dried in an oven at 120 °C overnight under nitrogen flow. The reaction was then carried out at 120 °C and 20 bar for 2 hours.

Nevertheless, DuPont, which is the manufacturer of Amberlyst CH28 catalyst used in the present project, recommends an activation protocol in which both hydrogen and deionized water need to flow through the catalytic bed for at least 16 hours [34]. The step by step activation procedure consists of the following steps:

1. Add deionized water at 0.5 bed volume/h and recirculate the water in the reactor.
2. Increase the reactor pressure to 30 bar with hydrogen.
3. Increase the reactor temperature to 90 °C at 10 °C/h.
4. Maintaining the reactor temperature, hold this status a minimum of 16 hours.
5. Stop the addition of deionized water and change the operational parameters to those relative to the reaction.

It must be mentioned that the catalyst supplier recommends this activation protocol for the hydrogenation of acetone to produce MIBK. Since the purpose of the present project is to perform the LA hydrogenation to produce GVL using this same catalyst, the recommended steps for the catalyst activation have been adapted to the studied reaction.

6. START-UP OF THE EXPERIMENTAL SETUP

6.1 MATERIALS

In Table 6, all the reactants used in the present work are listed along with their properties [35-39].

Table 6: Reactants properties

	Levulinic Acid	Hydrogen	Deionized water
CAS number	123-76-2	1333-74-0	7732-18-5
Chemical formula	$C_5H_8O_3$	H_2	H_2O
State at room temperature	White crystalline solid	Gas	Liquid
Density [g/cm^3]	1.13	0.0000899	1
Molecular weight [g/mol]	113.12	2.016	18.02
Melting point [°C]	33 - 35	-259.2	0
Boiling point [°C]	245 – 246	-253	100
Flash point [°C]	98	Not applicable	Not applicable
Purity	>98 %	>99.999 %	-
Supplier	Fisher Scientific A.G.	Abelló-Linde	-
Safety pictograms			None

In addition, other substances that are potential products or by-products of the studied reaction that were used as calibration standards (see Appendix 1) are specified in Table 7 [40-44].

Table 7: Properties of the substances used as calibration standards

	Gamma-Valerolactone	**Valeric Acid**	**Angelica Lactone**
CAS number	108-29-2	109-52-4	591-12-8
Chemical formula	$C_5H_8O_2$	$C_5H_{10}O_2$	$C_5H_6O_2$
State at room temperature	Liquid	Liquid	Liquid
Density [g/cm^3]	1.05	0.939	1.092
Molecular weight [g/mol]	100.12	102.13	98.10
Melting point [°C]	-31	(-20) - (-18)	13-17
Boiling point [°C]	207 - 208	185	55-56
Flash point [°C]	96	86	68
Purity	99 %	≥ 99 %	98 %
Supplier	Sigma-Aldrich Química, S.A.	Sigma-Aldrich Química, S.A.	Sigma-Aldrich Química, S.A.
Safety pictograms	None		

In order to pressurize the reactor and to detect possible leaks from the reactor, Nitrogen was used when needed (99.9995% purity, Abelló Linde).

Helium (99.998 % purity) was used as the carrier gas in the Gas Chromatograph (GC) analyses.

As mentioned before, (see Section 5.1) the catalyst used in this project is Amberlyst CH28, which is a bifunctional Pd-doped cation exchange commercial resin.

Lastly, the reaction bed was composed by a mixture of catalyst and silicon carbide (SiC) powder. Properties of silicon carbide are listed in Table 8 [45, 46].

Table 8: Silicon Carbide properties

CAS number	409-21-2
Molecular weight [g]	40.096
Melting point [°C]	2700
Density [g/mL]	3.16
Coarse	Grit 46
Supplier	CYMIT Quimica SL
Safety pictograms	

6.2 APPARATUS MODIFICATIONS

The initial setup (see Figure 8) was a commercial Microactivity-Reference unit. This unit is a modular, automatic and computer-controlled laboratory reactor designed to study catalytic reactions.

Figure 8: Microactivity-Reference, an HPLC pump and a computer

The basic unit configuration consists of:

- A tubular reactor with a 20 µm porous plate and L=300 mm.
- A reactive system integrated within a hot box, Tmax = 200 °C.
- A 6-port VICI valve for the reactor bypass.
- A high pressure Gas/Liquid separator.
- 2 gas inlets, one for Nitrogen and another one for Hydrogen.
- A HPLC Gilson liquid pump, 400 bar, from 0.1 to 5 mL/min.
- The system pressure, the level of liquid in the separator, the temperature of the hot box, and the temperature of the reactor are software-controlled.
- A software *Process@* for monitoring and data acquisition with distributed control.

Initial setup configuration is shown in Figure 9:

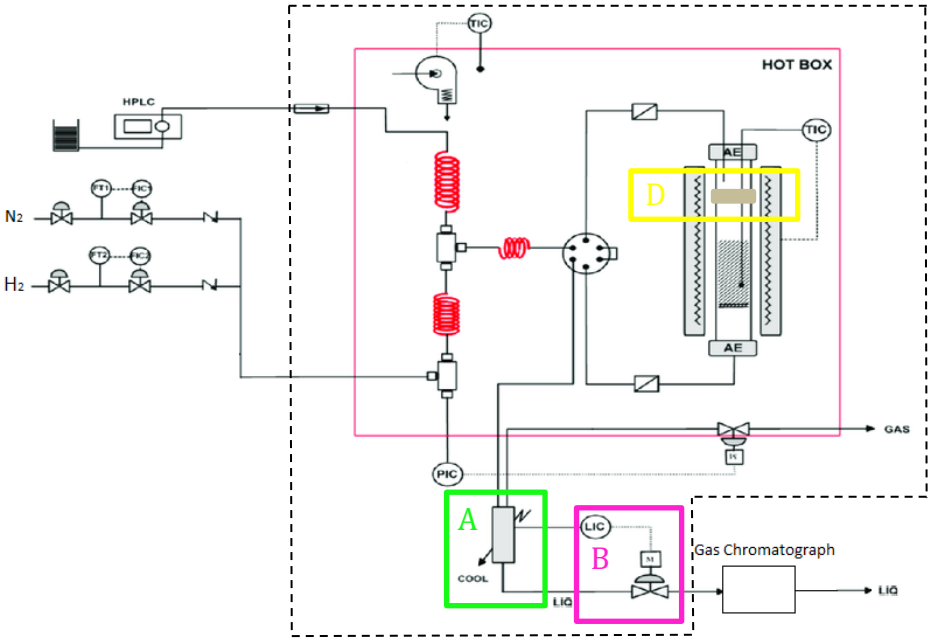

Figure 9: Initial configuration for Microactivity-Reference

The part surrounded by the dashed line is part of the Microactivity-Reference apparatus shown in Figure 8.

It should be noted that initially the samples from the outlet pipe were injected automatically to the GC using the automatized software.

The configuration of the Microactivity-Reference was not adequate to reproduce the studied reaction of the present project, since the facility was adapted to work by feeding two liquid reactants (one of them as a liquefied gas), instead of a liquid reactant and a permanent gas.

Starting from that initial unit configuration, a series of modifications were done to be able to develop the hydrogenation reaction of levulinic acid into gamma-valerolactone, those modifications are listed below:

- The separator that was included in the Microactivity-Reference apparatus was disabled since it did not work appropriately due to the high pressures reached that made the liquids go through the gas outlet pipe. In its place an outside gas scrubber bottle was installed. See frame A in Figure 9 and 10.
- In relation to the previous point, the separator level controller was also disabled since it no longer served any purpose. See frame B in Figure 9.
- A manual valve was installed at the outlet pipe in order to take the samples that would later be injected into the Gas Chromatograph. See frame C in Figure 10. This action could no longer be done automatically since the initial configuration was designed for pressurized liquids only, instead of mixed gas and liquid components. Therefore, gas-liquid phase separations could occur prior to GC injection, which ultimately resulted in undesired low GC analysis reproducibility.
- A thicker porous plate was placed in the upper part of the reactor because the one that was previously installed was very thin and, because of the space that remained between the thermocouple and the porous plate, the bed could come out towards the pipeline, potentially causing damage to other components downstream. See frame D in Figure 9 and 10.

The final layout of the apparatus for the hydrogenation of levulinic acid with the aforementioned modifications is shown in Figure 10.

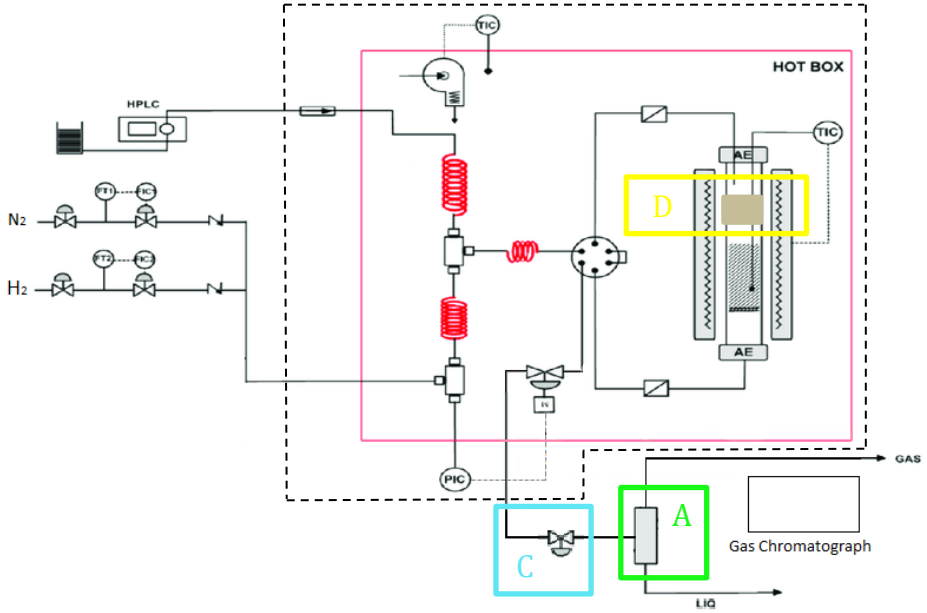

Figure 10: Final configuration for Microactivity-Reference

Thereafter, the final experimental setup for the present project consists of a Microactivity-Reference reactor connected to a gas bottle separator. The liquid is injected manually into a Gas Chromatograph that works as an analytical system. As shown in Figure 11, there is also a computer to analyze the results obtained.

Figure 11: Final experimental setup. From left to right: Microactivity-Reference reactor, gas bottle separator, GC and the computer.

As mentioned above, a computer with the software *Process@* was used for monitoring the data acquisition with an automatized control of the reaction parameters. A second computer is also connected to the GC, which is be able to obtain the analysis data. For the hydrogenation reaction of LA studied in this project, the set control parameters are listed in Table 9.

Table 9: Set control parameters for LA hydrogenation

	Acronym	Presure	Hot box temperature	Reactor temperature
Set Point	SP	20	100	130
Proportional control	P	200	15	60
Integral control	I	10	350	400
Derivative control	D	0	50	50
Upper limit of actuator action	MH1	90	95	30
Lower limit of actuator action	ML1	0	0	0
Upper limit of the field output signal	SLH	100	200	120
Lower limit of the field output signal	SLL	0	0	0

6.3 ANALISYS METHOD DEVELOPMENT

A Gas Chromatograph has been used in order to identify each substance present in the system.

In chromatography, each substance present in a sample will be separated by partition, will emerge from the column at different elution times and will go through a detection system that registers them. These times are known as the retention times. Each substance has a particular retention time (RT) depending on the type of sample and the proportion in it.

A Network GC System 6890N from Agilent Technologies Gas Chromatograph has been used. The separation has been carried out on a 50 m CP column with an inner diameter of 0.2 mm (HP-PONA 50m x 0.2mm x 0.5µm). Elution has been established by Helium at flow rate of 1 mL/min. The total analysis time has been 20 minutes, with an interval between each analysis of approximately 10 minutes, for the column temperature to return to its initial point.

Figure 12 shows the temperature profile configuration for the column during each analysis for the hydrogenation of LA.

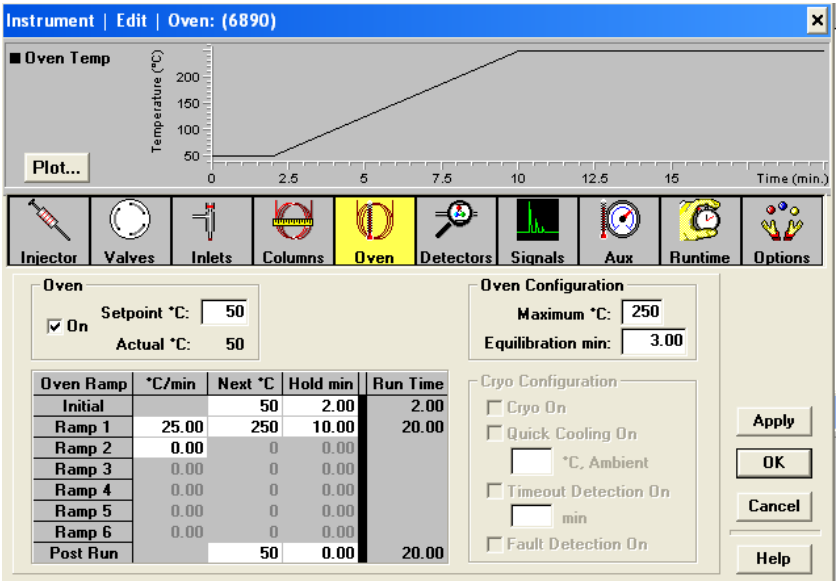

Figure 12: GC column temperature profile

Chromatograms represent the detector response in the *y* axis and the retention time in the *x* axis. They are made up of chromatographic peaks (see Figure 13). Those peaks refer to each component present in the sample. The GC area of every peak will change within samples because it is proportional to the relative mass amount of the substance present.

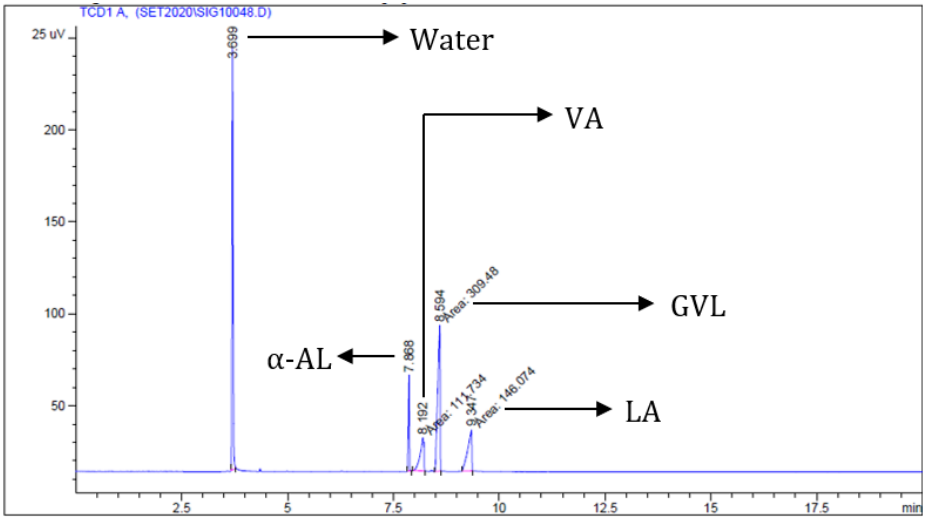

Figure 13: Example of a chromatogram for the conversion of LA to GVL

Firstly, a solution of all substances present in the reaction was injected. Typical RT of the substances present in the reaction studied are summarized, in order from lower to higher RT, in Table 10.

Table 10: Retention time for the components of the catalytic reaction of LA into GVL

Compound	Retention time [min]
Water	3.7
α-Angelica Lactone	7.89
Valeric acid	8.31
GVL	8.56
Levulinic acid	9.34

In the present experimental setup, the GC injections were done manually using a 1 µL volume syringe. The volume injected was 0.2 µL.

Then, in order to know the proportionality relationship between the relative area and the relative mass amount of each component, 14 different calibration vials were prepared. These 14 vials were prepared knowing the wt. % of each substance present (see Appendix 1). For every vial, 3 replicates were made to be able to determinate the experimental error and the variance of the results. Each component in the reaction studied in the present project has been calibrated in a wt. % range where it is thought that the results of the experimental procedure will be at.

The detector response gave the % of area under each peak, then, knowing which wt. % was related to that response, the calibration equations for each substance could be done. Table 11 summarizes all calibration equations for the hydrogenation reaction of LA and their associated R squared.

Table 11: Calibration equations for LA hydrogenation

Compound	Calibration equation	R^2
LA	$y = (1.209 \pm 0.027)\cdot x - (0.0023 \pm 0.0004)\cdot x^2$	0.999
Water	$y = (0.673 \pm 0.027)\cdot x + (0.0032 \pm 0.0004)\cdot x^2$	0.999
GVL	$y = (1.007 \pm 0.0096)\cdot x$	0.999
α-AL	$y = (1.156 \pm 0.017)\cdot x$	0.997
VA	$y = (1.25 \pm 0.057)\cdot x - (0.0123 \pm 0.0037)\cdot x^2$	0.998

The *y* value in the calibration equations represents wt. % and the *x* value represents the % area below the chromatograph peak. All calculations made for this calibration and data tables related are specified in Appendix 1.

7. STANDARD OPERATING PROCEDURES (SOPs) DEVELOPMENT

Standard Operating Procedures (SOPs) for the setup used to study the hydrogenation reaction of LA can be found in this section.

7.1 CATALYST ACTIVATION SOP

The catalyst activation SOP has been developed based on the catalyst activation method recommended by the supplier (DuPont) for the acetone hydrogenation reaction.

For the first step, the previous experiments from Nicol and Du Toit [29] were reproduced in the lab by adapting our experimental device to the activation method and experimental protocol proposed by the authors. However, since the results were not satisfactory, other sources of information were retrieved for comparative purposes. For instance, in the experiments reported by Talwalkar and Mahajani [27], Prinslo et al. [30] and Käldström et al. [32] with Amberlyst CH28 (see Section 5.2), no clear separation was established between activation and catalytic activity test protocols. This fact was deemed inadequate because the time devoted to activate the catalyst was considered an important process variable for further studies. In order to differentiate those times and to be able to carry out future optimization studies of the activation protocol, it has been decided to adapt the activation method specified by the catalyst supplier [34].

A catalyst pre-treatment consisting of a previous catalyst drying in the oven, has been specified in this SOP in order to ensure the removal of free and bounded water molecules from the catalyst sample. This way, the weight of catalyst weighted at *Step 2* will be as accurate as possible.

Also, from Moulijn [51] and Berger [52] previous studies, it has been decided to choose a perfectly mixed distribution of the bed particles, since they obtained the highest conversions with completely mixed particle mixtures.

Although, it has to be mentioned that a catalyst-to-inert dilution ratio (RD) of 10 (on weight basis) has been fixed. The catalyst dilution has been demonstrated to improve the temperature distribution and, consequently, reduces heat generations at critical points inside the reactors [53]. Also, using less catalyst and filling the empty spaces from the reactor with inert particles, will mean a lower catalyst use and a lower global cost. It has been proved that by using 5 grams of SiC and 0.5 grams of catalyst the reactor is not completely full, so that the particles can expand in contact with water (as can be seen in Table 5) and the thermocouple can fit too.

From the catalyst characterization (see Table 5 from Section 5.1) it has been shown that the diameter of the pores and the true swollen polymer volume are bigger in wet conditions; since this can assist to the contact between the reactants and the active sites of the catalyst, water is introduced into the reactor during activation.

In the DuPont recommended activation method, a 0.5 bed volume/h feed flow is needed. According to the 5 mL volume reactor used in this project, a 2.5 mL/h water feed flow would be needed. As mentioned in Section 6.2, an HPLC Gilson liquid pump is available in this experimental setup. Since the minimum flow available is 0.1 mL/min, this value has been set even though it is higher than the 0.042 mL/min required.

The supplier does not set any specific value for the hydrogen flow rate in the catalyst activation method recommended. This is because the hydrogen needed to increase the system pressure up to 30 bar is more than enough to reduce the catalyst Palladium. The minimum hydrogen value necessary for the reduction of the Palladium present in the bed has been calculated (see Appendix 3), this value will be the minimum that the catalyst should receive. Since it is a three-phase system (the catalyst is in the solid state, the water in the liquid state and the hydrogen in the gas state), the resistance of the hydrogen gas through the liquid phase to reach the surface of the catalyst will be high. That is why the solubility of hydrogen in water has been used as a limiting value. Since the hydrogen solubility in water is very low (see Appendix 3), the hydrogen must be in excess. For all these reasons, a 100 mL/min hydrogen feed flow has been set. Note that the relationship between water and hydrogen feed flows should be optimized in future works in order to reduce the operation time.

For more information about all these calculations, see Appendix 3.

Considering all the considerations explained above, the SOP is described below.

Step 1: CATALYST PRE-TREATMENT.

- Put a sufficient amount of catalyst in a porcelain crucible and place it in an atmospheric oven at 110 °C for at least 24 hours.

Step 2: BED CONFORMATION.

- Using a watch glass and a laboratory scale (scale precision used of 0.01 g), weigh 5 grams of SiC and 0.5 grams of Amberlyst CH28 previously pre-treated.

Step 3: REACTOR LOADING.

- Place the reactor upright in a plate foot stand (see Figure 14).
- Using two 10 mm open end wrench, unscrew the hex head bolts from the top part of the reactor (see n.1 in Figure 14). An adjustable wrench or a 10 mm socket spanner can also be used.
- Remove the top of the reactor carefully not to damage the thermocouple.
- Take out the porous plate and the copper ring and place t hem on a filter paper.
- Prepare a funnel with filter paper.
- Insert the bed conformed in Step 2 using the funnel and a spatula into the reactor, make sure it is well mixed.
- Put the porous plate and the copper ring back in place and close the reactor again.
- Put the six hex head screws in place and screw them in. Two 10 mm open end wrench, adjustable wrench or 10 mm socket spanner can be used.

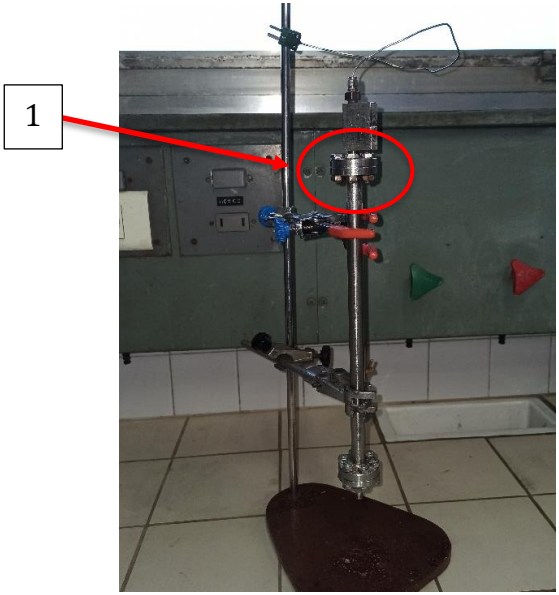

Figure 14: Reactor in a plate foot stand

Step 4: REACTOR ASSEMBLY.

- Insert the reactor into the heating jacket of the hot box.
- Screw the upper reactor outlet pipe to the thermocouple head (see n.1 in Figure 15). Use an adjustable wrench and a 13 mm open end wrench.
- Screw the lower inlet pipe to the bottom part of the reactor. Use two 11 mm open end wrenches (see n.2 in Figure 15).
- Plug the thermocouple male plug into the female socket inside the hot box. It is necessary to mention that the wide part of the male plug must be placed on the right side of the female plug.
- Turn on the Microactivity-Reference power button (see Figure 15).

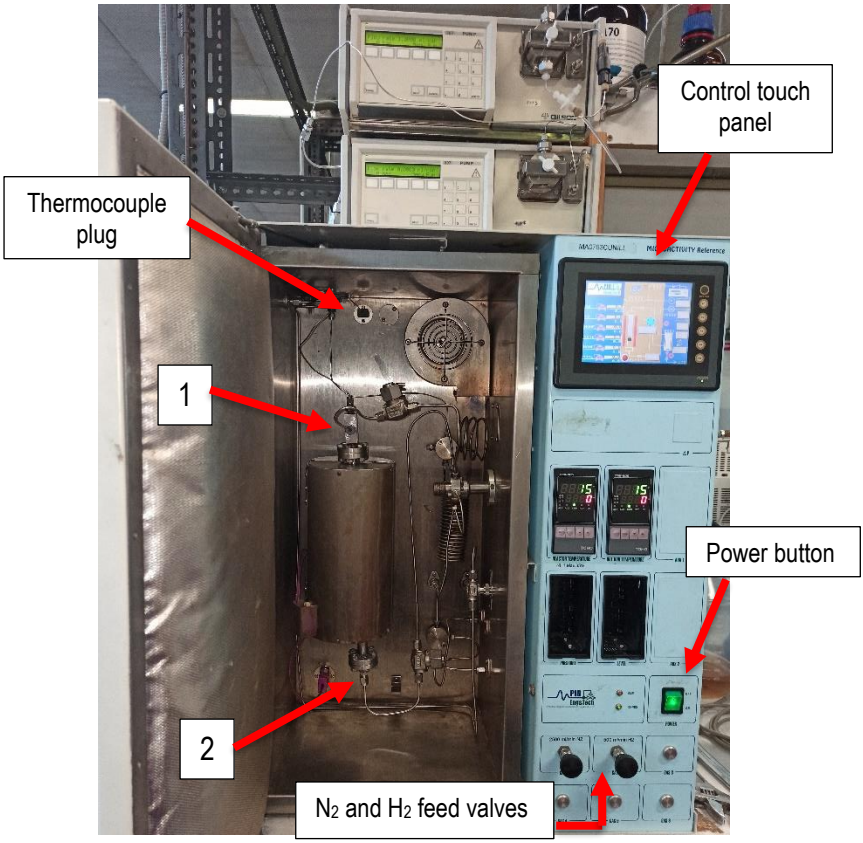

Figure 15: Reactor assembly inside the Hot Box

Step 5: LEAK TEST.

- Open nitrogen and hydrogen feed valves (see Figure 15).
- Make sure that the three way stopcock of the liquid feed to the pump is positioned so that it allows the deionized water to pass through and not the LA solution. If necessary, refill the water bottle.
- Using a syringe, make sure there are no air bubbles in the feed line to the pump to avoid cavitation.
- Using the control touch panel from the Microactivity-Reference (see Figure 15) activate the bypass valve.

- Using the pump panel or the software *Process@* in the computer (see Figure 16), set the liquid pump flow value at 3 mL/min. Wait until water comes out from the reactor outlet pipe (10 minutes approximately).

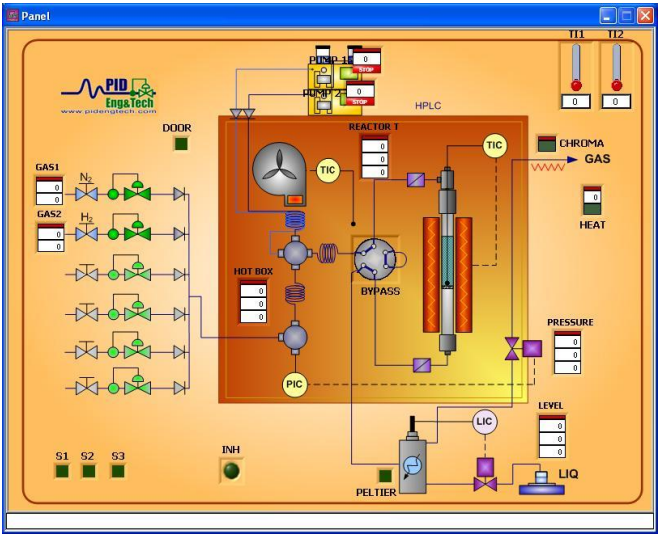

Figure 16: Software *Process@* panel

- Turn off the liquid pump and deactivate the bypass valve.
- Using either the computer software *Process@* installed or the control touch panel in the Microactivity-Reference, set the parameters indicated in Table 12.

Table 12: Leak test conditions

Liquid pump flow [mL/min]	0.2
Nitrogen flow [mL/min]	150
Pressure SP [bar]	40

- Wait at least 30 minutes and make sure no joint has any leak. Use soap solution to check for leaks. If needed, screw the leaking joints tighter.
- Once no leaks are spotted, turn off the pump and reset all parameters to zero.

Step 6: CATALYST ACTIVATION.

- Turn on the liquid pump and set its set point (SP) to 0.1 mL/min and recirculate the deionized water in the reactor.

- Set the pressure SP at 30 bar and the hydrogen flow rate up to 100 mL/min. Note that if the pressure does not stabilize or does not reach 30 bar, it may be necessary to turn on the nitrogen feed flow at 50 mL/min.
- When the pressure is stablished, increase the reactor temperature to 90 °C with a heating ramp of 10 °C/h.
- At the same time, increase the hot box temperature to 80 °C with a heating ramp of 10 °C/h.
- Maintain all the set parameters during, at least, 16 hours.

7.2 ACTIVITY TEST SOP

The catalyst activity test SOP for the hydrogenation reaction of LA has been developed based on Nicol and Du Toit [29] previous experiment with Amberlyst CH28. However, some differences have been enclosed in order to adapt the protocol to the experimental device used in the present project. Note that Nicol and Du Toit studied the synthesis of MIBK by acetone hydrogenation.

As the reactor used by Nicol and Du Toit [29] was much larger than the reactor in our experimental device, all flow, volume and mass values had to be scaled down. A linear hourly space velocity (LHSV) of 4 has been taken as a reference for this downscaling. These researchers performed their experiment with four different LHSV of 4, 6, 8 and 16 h^{-1}, but due to the restrictive volume of the reactor in the present experimental setup, a value of 4 has been chosen.

Gutierrez [49] and Martinez [50] previous projects relationship between wet and dry catalyst volume has been taken as a reference (see Appendix 3). Setting a RD of 10 and loading 0.5 grams of catalyst to the reactor, a 0.102 mL/min feed flow is needed to work with a LHSV of 4. A 50% wt. of LA feed solution has been chosen to ensure the water presence in the reactor for the catalyst pores to be in its larger form.

Nicol and Du Toit [29] used a 1.1 molar ratio, between hydrogen and acetone feeds, for the experiments performed. Taking this value as a reference, the hydrogen flow required for this experiment is 4.1 mL/min. Due to device restrictions, a value of 50 mL/min has been set since at lower hydrogen flow rates the system pressure did not stabilize correctly. In order to reach the operating pressure of 30 bar, a 100 mL/min nitrogen flow is needed too.

The operating temperature has been fixed at 130 °C. Even though Nicol and Du Toit [29] also performed some experiments at 140 °C and 150 °C, the maximum operating temperature for Amberlyst CH28 according to its safety data sheet [33] is 130 °C.

For more information about all these calculations, see Appendix 3.

Taking into account the considerations explained above, the SOP is described below.

Step 1: ACTIVITY TEST.

- Maintain the pressure and both the reactor and the hot-box temperatures SP values (that is, 30 bar, 90 °C for the reactor temperature, and 80 °C for the hot box temperature).
- Turn off the liquid pump and the hydrogen feed flow.
- Change the three way stopcock of the liquid feed to the position so that it allows the 50 % wt. LA solution to pass through instead of the deionized water. If necessary, refill the 50 % wt. LA solution bottle before.
- Using a syringe, make sure there are no air bubbles in the feed line to the pump to avoid cavitation.
- Using the liquid pump panel or the software *Process@* in the computer, set the pump flow value at 0.1 mL/min.
- Wait for 30 minutes approximately until the LA solution has displaced the deionized water.
- Meanwhile, heat up the reactor to the operating temperature (130 °C) with a heating ramp of 5 °C/min. Heat up the hot box temperature SP to 100 °C with a heating ramp of 5 °C/min too.
- When the operating temperature is accomplished, turn on the hydrogen and nitrogen feed to 50 mL/min and 100 mL/min, respectively.
- Maintain this set parameters at least 4 hours.

* In order to stablish the steady state condition, samples have to be taken and injected into de GC every 30 minutes (see below).

- Using a 11 mm open end wrench and an adjustable wrench, unscrew the hex nut cap from the three-way union of the outlet reactor pipe to the G/L separator.

- Collect a sample of approximately 1 mL of the outlet flow.
- Screw back the hex nut cap to the three-way union.
- Set the GC in *LA_inj_M.M* mode and press the *Pre-Run* button from the GC panel. Wait until *Ready* appears in GC panel.
- Using a 1 µL volume syringe, inject 0.2 µL of the sample into the GC. Simultaneously, press the *Run* button to start the method.
- Repeat these steps every 30 minutes to characterize the reactor outlet composition of the liquid phase. When three or more GC analyses show the same composition, within the experimental error margin, it can be stated that the steady state has been reached.

Step 2: EQUIPMENT STOP.

- Turn off the liquid pump and both, nitrogen and hydrogen, flows.
- Using either the computer *Process@* software installed (see Figure 16) or the control touch panel in the Microactivity-Reference (see Figure 15), reset the pressure and temperatures SP to zero.
- Turn on the bypass valve.
- Set the GC in *STAND_BY* mode.
- Wait until pressure and temperatures reach room conditions.
- Turn off the bypass valve.

Step 3: CLEAN UP.

- Turn off the Microactivity-Reference power button (see Figure 15).
- Unplug the thermocouple from the hot box plug.
- Unscrew the lower inlet pipe from the bottom part of the reactor. Use two 11 mm open end wrenches.
- Unscrew the upper reactor outlet pipe from the thermocouple head using an adjustable wrench and a 13 mm open end wrench.
- Place the reactor upright in a plate foot stand (see Figure 14).
- Using two 10 mm open end wrench, unscrew the hex head bolts from the top part of the reactor. An adjustable wrench or a 10 mm socket spanner can also be used.
- Remove the top of the reactor carefully not to damage the thermocouple.
- Take out the porous plate and the copper ring and place them on a filter paper.

- Inject pressurized air through the bottom of the reactor so that the particle bed is expelled over a glass container.
- Fill the reactor with water and inject compressed air through the bottom part of the reactor again. Perform this step repeatedly until no catalyst particles remain inside the reactor.
- If necessary, place the copper ring, the porous plate and the screws in a glass container with acetone and in an ultrasound bath to clean them.

7.3 AUTOMATED METHOD

Using the *Process@* software, control sessions can be created, which allow the operation to be carried out in an automated way. For the studied reaction, from the Catalyst Activation SOP, *Step 6* can be carried out in an automated way, allowing less time investment for the operator while ensuring reproducibility of reaction conditions. Other steps, such as the leak test, requires different operation times depending on the leaks detected in the equipment during each run and are therefore to be performed by an operator.

However, the catalyst activation and the activity test cannot be performed in a single session since the Microactivity-Reference reactor must be stopped due to the need to change the fluid fed to the reactor manually.

To access the control sessions, the following steps may be followed:

- Open the *Process@* program installed in the computer.
- From the upper toolbar, select the icon "*Sessions*".
- In the window displayed, select the option "*Configure Sessions*".

The session configuration panel will immediately be displayed. In order to perform the catalyst activation and its activity test, the following sessions values (see Figure 17 and Figure 18) have to be reproduced.

The possibility to automate a process is a very important aspect in a project in which reproducibility is desired, due to the possibility of maintaining or changing the parameters of the system values without the need for an operator to do so. For long work sessions, such as the proposed activation protocol that lasts at least 16 hours, it is important to be able to work with an automated system.

Notice that if any change is made in any process value in future projects, it should also be changed in these sessions if working in an automated way is desired.

			Session 1	Session 2	Session 3	Session 4	Session 5	Session 6
Alias			Session 1	Session 2	Session 3	Session 4	Session 5	Session 6
Description			Stabilization	Hydrogen	Increase T	Activation	Stabilization	
SessionTime (min)			10	15	450	960	99999	-
Conditional Jump?			×	×	×	×	×	×
Control Parameter								
Operator								
Value								
Next Session #			2	3	4	5	End	End
✓	BYPASS	BYP						
✓	DOOR	PUE						
✓	GAS1	MF1		50			50	
✓	GAS2	MF2		100			15	
✓	HOT BOX	SV1	0		80			
✓	HOT BOX	P1	15					
✓	HOT BOX	I1	350					
✓	HOT BOX	D1	50					
✓	HOT BOX	RP1	0		0.17			
✓	PRESSURE	SV1	0	30				
✓	PRESSURE	P1	200					
✓	PRESSURE	I1	15					
✓	PRESSURE	D1	0					
✓	PRESSURE	RP1	0					
✓	PUMP 1	C		0.1			0	
✓	PUMP 1	R						
✓	REACTOR T	SV1	0		90			
✓	REACTOR T	P1	60					
✓	REACTOR T	I1	400					
✓	REACTOR T	D1	50					
✓	REACTOR T	SLH	150					
✓	REACTOR T	RP1	0		0.17			

Figure 17: Catalyst activation control session

Column referred as *Session 5* has been configured so that the reactor maintains a reducing atmosphere (reducing the hydrogen flow and adding nitrogen). The pump is also turned off in this step. The 99999 minutes of this step are symbolic so that the experimental device can be left from one day to the next and when returning to the laboratory, the session still continues to control.

			Session 1	Session 2	Session 3	Session 4	Session 5	Session 6
Alias			Session 1	Session 2	Session 3	Session 4	Session 5	Session 6
Description			Stabilization	Conditioning	Test	Stop	Clean	--
SessionTime (min)			10	30	240	120	9999	
Conditional Jump?			×	×	×	×	×	×
Control Parameter								
Operator								
Value								
Next Session #			2	3	4	5	End	End
✓	BYPASS	BYP				1	0	
✓	DOOR	PUE						
✓	GAS1	MF1	50		100	0		
✓	GAS2	MF2	15		50	0		
✓	HOT BOX	SV1	80	100		0		
✓	HOT BOX	P1	15					
✓	HOT BOX	I1	350					
✓	HOT BOX	D1	50					
✓	HOT BOX	RP1		5		0		
✓	PRESSURE	SV1	30			0		
✓	PRESSURE	P1	200					
✓	PRESSURE	I1	15					
✓	PRESSURE	D1	0					
✓	PRESSURE	RP1	0					
✓	PUMP 1	C		0.1		0		
✓	PUMP 1	R						
✓	REACTOR T	SV1	90	130		0		
✓	REACTOR T	P1	60					
✓	REACTOR T	I1	400					
✓	REACTOR T	D1	50					
✓	REACTOR T	SLH	150					
✓	REACTOR T	RP1		5		0		

Figure 18: Activity test control session

For this control session (Figure 18), the column named as *Session 5* refers to the last step listed in the Activity Test SOP. The 9999 minutes are symbolic so that it gives enough time for the equipment conditions to reach room conditions.

8. START-UP DEMONSTRATION

As previously mentioned, all the experiments that have been carried out to ensure the right start-up of the experimental device were carried out following the Activity Test SOP adapted from Nicol and Du Toit [29] activation method; since the main purpose of those experiments was not to study the activation process itself but the start-up of the laboratory device. Since results were not deemed as satisfactory, in terms of studying the catalyst activation and, subsequently, the hydrogenation reaction of LA, a new Catalyst Activation SOP was developed based on the activation method proposed by the supplier (see Section 5.2).

In order to develop the SOPs, many trial experiments have been carried out in order, firstly, to ensure the correct operation of the installation, and secondly, to draft the procedure that ensures an optimal result of the studied reaction.

The experiments carried out show that the installation works correctly, that there are no leaks in the system and that the working parameters are maintained over time. The laboratory setup is now suitable for carrying out the hydrogenation reaction of levulinic acid in future studies.

In Table 13 are listed all the experiments carried out successfully that prove the correct operation of the equipment. Previous trials have not been included in the table.

Table 13: Experiments performed

	Run 1	**Run 2**	**Run 3**	**Run 4**	**Run 5**
50 % wt. LA solution [mL/min]	0.2	0.2	0.2	0.2	0.2
Catalyst weight [g]	1	1.07	1.02	1.01	1.03
SiC weight [g]	0.53	0.52	0.53	0.55	0.51
Pressure [bar]	20	20	20	40	30
Reactor temperature [°C]	130	130	130	130	130
Hydrogen [mL/min]	50	50	100	100	100
Nitrogen [mL/min]	0	0	0	0	0
Experimental time [h]	5.5	7.5	4.5	6	4

For *Run 5* (see Table 13), a previous batch catalyst activation was made in the same tubular reactor. It was filled with water and the pressure was raised to 30 bars with hydrogen and left for 23 hours with all inlets and outlets pipes closed. No leaks were observed since after 23 hours the 30 bars of pressure were maintained. The automated control of the equipment allowed to work the 23 hours straight.

As mentioned before, several experiments have been successfully carried out in an automated way with the software *Process@* program. Figure 19 shows one of the graphs obtained in a start-up experiment performed. As shown, the system is stable over time and stabilizes correctly after a disturbance in any process parameter.

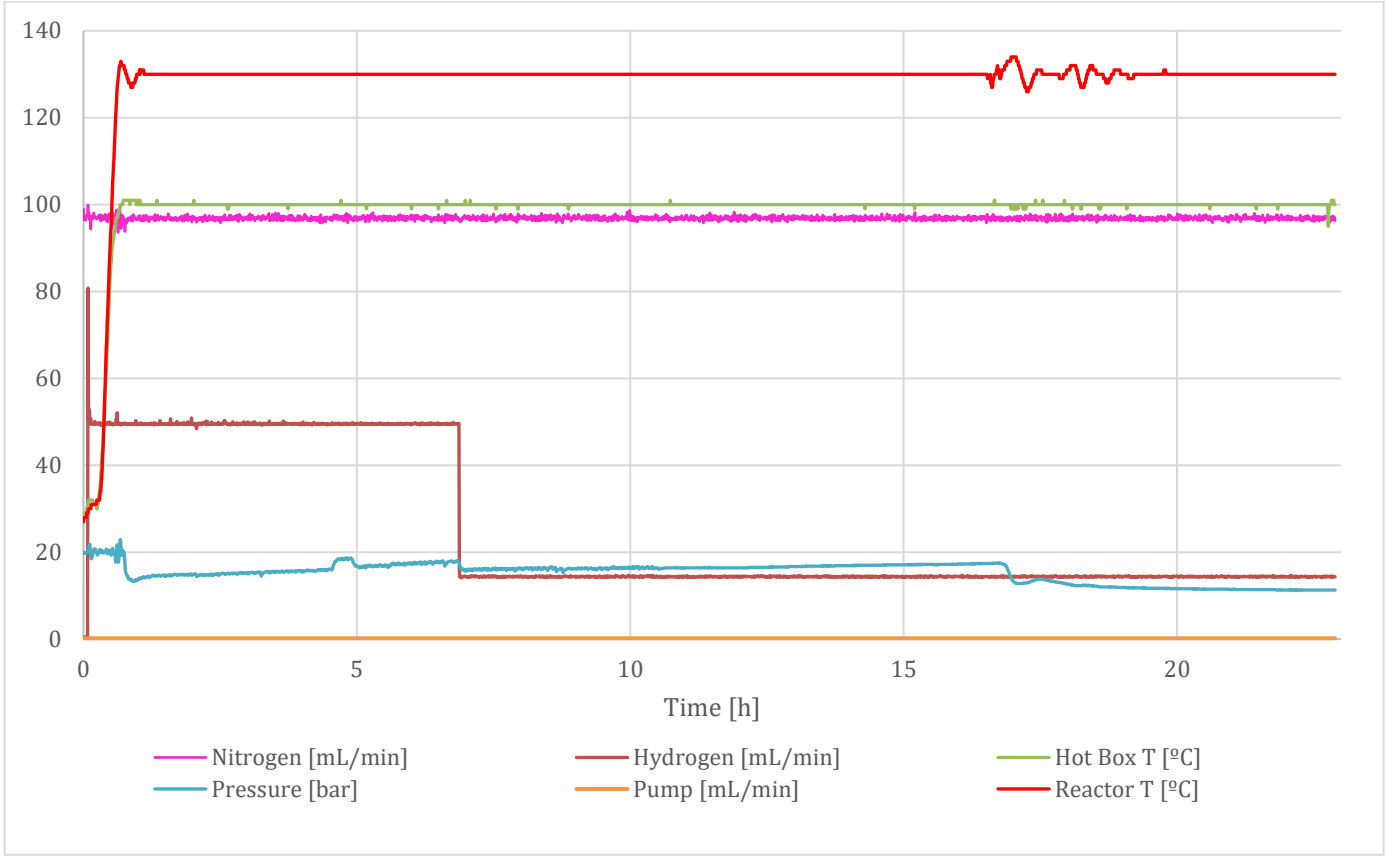

Figure 19: Process values for a start-up experiment

9. CONCLUSIONS

Fuels and fuel additives from biomass origin are an increasingly real alternative to the use of fossil fuels. Levulinic acid obtained through the Biofine Process from lignocellulose is a value chemical platform product. LA can produce gamma-valerolactone, which is widely used as a precursor to many value-added products, such as fuel additives. The production reaction of GVL by hydrogenation of LA has been the reaction studied in the present project.

With the aim of being able to carry out this reaction, the adaptation of an existing commercial installation of Microactivity-Reference was in order. The necessary modifications have been made so that the installation works properly and the working method is correct. This has allowed me to learn more about installations and to see the more technical part of the device. It has allowed me to be more multidisciplinary and to be decisive with the mishap I was encountering. It has made me apply all the knowledge acquired throughout the four years of the degree to be able to adapt an existing installation to work for a specific reaction.

At the same time, I calibrated the analysis system in order to find the calibration equations for each compound in the reaction and to be able to relate the signal obtained by the GC with the amount of relative mass referred to for each compound in the samples. I have been able to see the evolution of the signal received by the GC in real time and to predict and understand how the signal changed according to the sample that was injected. Due to the need to clean the entire installation, I was able to see all the parts of the GC and learn how they work.

Secondly, correct automatic control by the control software has been achieved, as well as the correct operation of the system in light of any disturbance in the parameters. Working on this field, I have been able to see and predict how the parameters of the control software could make the response to a disturbance change.

Finally, in order to carry out future projects and investigations of this reaction at this facility, SOPs for both the catalyst activation and the activity test methods have been drafted. These protocols have been written in a clear and understandable way so that anyone who ever want to reproduce this reaction in this experimental device can do so.

One of the possible fields of study in future projects would be the optimization of the activation protocol parameters. Study how the temperature, the hydrogen feed flow rate, the amount of catalyst and/or the dilution ratio can affect in the reaction yield.

REFERENCES AND NOTES

[1] Aro, E. M. From first generation biofuels to advanced solar biofuels; *Ambio*, **2016**, 45, 24-31.
[2] *Eurosat Statistics Explained* (**2019**). Primary production of liquid biofuels EU-28 1990-2017. <https://ec.europa.eu/eurostat/statistics-explained/index.php?title=File:Figure_6-Primary_production_of_liquid_biofuels_EU-28_1990-2017.png> (accessed Oct 28, 2020)
[3] *Statista* (**2020***)*. A.Díaz, Consumo de biodiesel España 2007-2019. <https://es-statista-com.sire.ub.edu/estadisticas/1034919/consumo-de-biodiesel-espana/> (accessed Oct 28, 2020)
[4] Banse, M., van Meijl, H., & Woltjer, G. The Impact of First and Second Generation Biofuels on Global Agricultural Production, Trade and Land Use (Presented at the 11th Annual Conference on Global Economic Analysis, Helsinki, Finland). *Purdue University*, **2008**, 6-9.
[5] Beltrán, J. U. H.; De Lira, I. O. H.; Santos, M. M. C.; Luevanos, A. S.; Terán, F. H.; Balagurusamy, N. Insight into Pretreatment Methods of Lignocellulosic Biomass to Increase Biogas Yield: Current State, Challenges, and Opportunities. *Appl. Sci.* **2019**, 9, 3721-3750.
[6] Hayes, D. J.; Ross, J.; Hayes, M. H. B.; Fitzpatrick, S. The Biofine Process: Production of Levulinic Acid, Furfural and Formic Acid from lignocellulosic feedstocks; *Biorefinery (8b)*, **2009**, 139-164.
[7] Dutta, S; Yu, I. K. M.; Tsang, D. C. W.; Ng, Y. H.; Ok, Y. S.; Sherwood, J.; Clark, J. H. Green synthesis of gamma-valerolactone (GVL) through hydrogenation of biomass-derived levulinic acid using non-noble metal catalyst: a critical review; *Chemical Engineering Journal*, **2019**, 372, 992-1006.
[8] Galletti, A. M. R.; Antonetti, C.; De Luise, V.; Martinelli, M. A sustainable process for the production of γ-valerolactone by hydrogenation of biomass-derived levulinic acid; *Green Chem.*, **2012**, 14, 688-694.
[9] Schuette, H. A.; Thomas, R. W. Normal valerolactone III its peparation by the catalytic reduction of levulinic acid with hydrogen in the precence of platinum oxide; *J. Am. Chem. Soc.* **1930**, 52(7), 3010–3012.
[10] Deng, L.; Zhao, Y.; Li, J.; Fu, Y.; Liao, B.; Guo, Q.Conversion of Levulinic Acid and Formic Acid into g-Valerolactone over Heterogeneous Catalysts; *ChemSusChem* **2010**, 3, 1172 – 117.
[11] Alonso, D. M.; Wettstein, S. G.; Dumesic, J. A. Gamma-valerolactone, a sustainable platform molecule derived from lignocellulosic biomass; *Green Chem.*, **2013**, 15, 584-595.
[12] Horváth, I. T.; Mehdi, H.; Fábos, V.; Boda, L.; Mika, L. T. Gamma-Valerolactone a sustainable liquid for energy and carbon-based chemicals; *Green Chem.*, **2008**, 10, 238–242.
[13] Horváth, I. T. Solvents from nature; *Green Chem.*, **2008**, 10, 1024–1028.
[14] Bereczky, A.; Lukács, K.; Farkas, M.; Dóbé, S. Effect of γ-Valerolactone Blending on Engine Performance, Combustion Characteristics and Exhaust Emissions in a Diesel Engine; *Natural Resources*, **2014**, 5, 177-191.
[15] Yan, K.; Yang, Y.; Chai, J.; Lu, Y. Catalytic reactions of gamma-valerolactone: A platform to fuels and value-added chemicals; *Applied Catalysis B: Environmental*, **2015**, 179, 292-304.
[16] Ye, L.; Han, Y.; Feng, J.; Lu, X. A review about GVL production from lignocellulose: Focusing on the full components utilization; *Industrial Crops and Products*, **2020**, 144, 112031.
[17] Geilen, F. M. A.; Engendahl, B.; Hölscher, M.; Klankermayer, J.; Leitner, J. Selective Homogeneous Hydrogenation of Biogenic Carboxylic Acids with [Ru(TriPhos)H]+: A Mechanistic Study; *J. Am. Chem. Soc.*, **2011**, 133, 14349–14358.

[18] Kumarvel, S.; Thiripuranthagan, S.; Durai, M.; Erusappan, E.; Vembuli, T.Catalytic transfer hydrogenation of biomass-derived levulinic acid to g-valerolactone over Sn/Al-SBA-15 catalysts; *New J. Chem*., **2020**, 44, 8209-8222.

[19] Li, W.; Xie, J.; Lin, J.; Zhou, Q. Highly efficient hydrogenation of biomass-derived levulinic acid to γ-valerolactone catalyzed by iridium pincer complexes; *Green Chem*., **2012**, 14, 2388-2390.

[20] Chalid, M.; Broekhuis, A. A.; Heeres, H. J. Experimental and kinetic modeling studies on the biphasic hydrogenation of levulinic acid to -valerolactone using a homogeneous water-soluble Ru–(TPPTS) catalyst; *Journal of Molecular Catalysis A: Chemical*, **2011**, 341, 14-21.

[21] Manzer, L. E. Catalytic synthesis of α-methylene-γ-valerolactone: a biomass-derived acrylic monomer; *Applied Catalysis A: General*, **2004**, 272, 249-256.

[22] Du, X. L.; Bi, Q. Y.; Liu, Y. M.; Cao, Y.; Fan, K. N. Conversion of Biomass-Derived Levulinate and Formate Esters into g-Valerolactone over Supported Gold Catalysts; *ChemSusChem*, **2011**, 4, 1838 – 1843.

[23] Sudhakar, M.; Kantam, M. L.; Jaya, V. S.; Kishore, R.; Ramanujachary, K. V.; Venugopal, A. Hydroxyapatite as a novel support for Ru in the hydrogenation of levulinic acid to γ-valerolactone; *ChemSusChem,* **2011**, 4, 1838 - 1843.

[24] Bourne, R. A.; Stevens, J. G.; Je, J.; Poliakoff, M. Maximising opportunities in supercritical chemistry: the continuous conversion of levulinic acid to γ-valerolactone in CO2; *Chem. Commun*, **2007**, 4632 - 4634.

[25] Son, P. A.; Nishimura, S.; Ebitani, K. Production of g-valerolactone from biomassderived compounds using formic acid as a hydrogen source over supported metal catalysts in water solvent; *RSC Adv*., **2014**, 4, 10525-10530.

[26] Upare, P. P.; Lee, J. M.; Hwang, D. W.; Halligudi, S. B.; Hwang, Y. K.; Chang, J. S. Selective hydrogenation of levulinic acid to γ-valerolactone over carbon-supported noble metal catalysts; *Journal of Industrial and Engineering Chemistry*, **2011**, 17, 287-292.

[27] Talwalkar, S.; Mahajani, S. Synthesis of methyl isobutyl ketone from acetone over metal-doped ion exchange resin catalyst; *Applied Catalysis A: General*, **2006**, 302, 140–148.

[28] *EcuRed* 3744458 (**2020**). Resina de intercambio iónico. <https://www.ecured.cu/index.php?title=Resina_de_intercambio_i%C3%B3nico&oldid=3744458> (accessed Nov 15, 2020)

[29] Nicol, W.; Du Toit, E. L. One-step methyl isobutyl ketone synthesis from acetone and hydrogen using Amberlyst CH28; *Chemical Engineering and Processing* **2004**, 43, 1539 – 1545.

[30] Prinsloo, N. M.; Engelbrecht, J. P.; Mashapa, T. N.; Strauss, M. J. Acetone to MIBK process optimization through multidisciplinary chemometrics and in-line NIR spectroscopy; *Applied Catalysis A: General*, **2008**, 344, 20–29.

[31] Trejo, J. A.; Tate, J.; Martenak, D.; Huby, F.; Baxter, S. M.; Schultz, A. K.; Olsen, R. J. State of the Art Bifunctional Hydrogenation Heterogeneous Polymeric Catalyst; *Top Catal*, **2010**, 53, 1156–1162.

[32] Käldström, M.; Lindblad, M.; Limminpää, K.; Wallenius, S.; Toppinen, S. Carbon Chain Length Increase Reactions of Platform MoleculesDerived from C5 and C6 Sugars; *Ind. Eng. Chem. Res*., **2017**, 56, 13356-13366.

[33] *Rohm and Haas Company* (**2003**). Lenntech Amberlyst CH28 safety data sheet; <https://www.lenntech.com/Data-sheets/Dow-Amberlyst-CH28-L.pdf> (accessed Oct 20, 2020)

[34] *Rohm and Haas Company* (**2004)**. Practical guide: Suggestions for catalyst Amberlyst CH28 loading and activation; <http://www.amberlyst.com> (accessed Oct 20, 2020)

[35] *ThermoFisher SCIENTIFIC* (**2020**). Levulinic acid safety data sheet; <https://www.fishersci.se/chemicalProductData_uk/wercs?itemCode=10607943&lang=EN> (accessed Dec 27, 2020)

[36] *Merck Millipore* (**2017)**. Levulinic acid safety data sheet 814254); <https://www.merckmillipore.com/ES/es/product/msds/MDA_CHEM-814254?Origin=PDP> (accessed Oct 20, 2020)

[37] *Lluch Essence* (**2018**). Levulinic acid safety data sheet); <http://www.lluche.com/es/productos/Pages/OpenDocuments.aspx?artNumber=100025700&type=3&template=00163QQQQH_L1_V5.doc&outFileName=100025700_L1_V5.pdf&productName=ACIDO%20LEVULINICO%2097%&reachNumber=--/--> (accessed Oct 20, 2020)
[38] *Linde* (**2020**). Hydrogen safety data sheet; <https://www.linde-gas.es/es/images/10021694.%20rev%202.3.%20Hidrogeno-Biogon%20H_tcm316-89784.pdf> (accessed Oct 20, 2020)
[39] *Praxair* (**2013**). Hydrogen safety data sheet; <https://www.ecosmep.com/cabecera/upload/fichas/9932.pdf> (accessed Oct 20, 2020)
[40] *Luch Essence* (**2018**). Gamma-valerolactone safety data sheet; <http://www.lluche.com/es/productos/Pages/OpenDocuments.aspx?artNumber=100115700&type=3&template=00764QQQQL_L1_V7.doc&outFileName=100115700_L1_V7.pdf&productName=GAMMA-VALEROLACTONA&reachNumber=--/--> (accessed Oct 20, 2020)
[41] *Restek* (**2017**). Gamma-valerolactone safety data sheet; <https://www.restek.com/documentation/msds/34080_euesp.pdf> (accessed Oct 22, 2020)
[42] *ThermoFisher SCIENTIFIC* (**2020**). Valeric acid safety data sheet; <https://www.fishersci.es/chemicalProductData_uk/wercs?itemCode=10686584&lang=ES> (accessed Dec 27, 2020)
[43] *TCI America* (**2018**). Angelica lactone safety data sheet; <https://www.tcichemicals.com/US/en/p/A1090> (accessed Oct 22, 2020)
[44] *Sigma-Aldrich* (**2018**). Angelica lactone safety data sheet; <https://www.sigmaaldrich.com/MSDS/MSDS/PleaseWaitMSDSPage.do?language=&country=ES&brand=ALDRICH&productNumber=A86406&PageToGoToURL=https://www.sigmaaldrich.com/catalog/product/aldrich/a86406?lang=es&region=ES> (accessed Oct 22, 2020)
[45] *Washington Mills* (**2015**). Silicon carbide safety data sheet; <https://www.washingtonmills.com/sites/default/files/2019-03/carborex_c-5_green_spanish.pdf> (accessed Oct 22, 2020)
[46] *ThermoFisher SCIENTIFIC* (**2019**). Silicon carbide safety data sheet; <https://www.fishersci.es/store/msds?partNumber=12387133&productDescription=500GR+Carborundum%2C+technical%2C+SLR%2C+powder%2C+medium%2C+about+165%C2%B5m+%2880+grit%29&countryCode=ES&language=es> (accessed Oct 22, 2020)
[47] Werpy, T; Petersen, G. Top value added chemicals from biomass: Results of Screening for Potential Candidates from Sugars and Synthesis Gas; *U.S Department of Energy*, **2004**, Volume I, 45-48.
[48] De Souza, R. O. M. A.; Miranda, L. S. M.; Luque, R. Bio(chemo)technological strategies for biomass conversion into bioethanol and key carboxylic acids; *Green Chem.*, **2014**, 16, 2386-2405.
[49] Gutierrez, E. Levulinic acid upgrade to γ-valerolactone by hydrogenation by using a bifunctional catalyst; *University of Barcelona*, **2020**.
[50] Martínez, H. Levulinic Acid Upgrade to γ-valerolactone Using a Bifuntional Catalyst; *University of Barcelona*, **2020**.
[51] Moulijn, J. A.; Ramírez, J. P.; Berger, R. J.; Hamminga, G.; Mul, G.; Kapteijn, F. High-throughput experimentation in catalyst testing and in kinetic studies for heterogeneous catalysis; *Catalysis Today*, **2003**, 81, 457-471.
[52] Berger, R. J.; Ramírez, J. P.; Kapteijn, F.; Moulijn, J. A. Catalyst performance testing: bed dilution revisited; *Chemical Engineering Science*, **2002**, 57, 4921-4932.
[53] Quina, M. M. J.; Ferreira, R. M. Q. Thermal Runaway Conditions of a Partially Diluted Catalytic Reactor; *Ind. Eng. Chem. Res.*, **1999**, 38(12), 4615–4623.
[54] Bozell, J. J.; Petersen, G. R. Technology development for the production of biobased products from biorefinery carbohydrates - The US Department of Energy's "Top 10" revisited; *Green Chem.*, **2010**, 12, 539-554.

[55] *Merck Millipore*. Intercambiadores iónicos ; Merck KGaA. <https://www.merckmillipore.com/ES/es/20131209_163012?ReferrerURL=https%3A%2F%2Fwww.google.com%2F> (accessed Dec 27, 2020)

[56] Lide, D. R. Physical Constants of Organic Compounds; *CRC Handbook of Chemistry and Physics*, **2005**, Internet Version, 1317-1318.

[57] Li, B.; Dong, W.; Ren, Y.; Feng, A. Preparation and characterization of spherical nickel-doped carbonized resin as hydrogenation catalysts: II. Thermal decomposition of resin and preparation of metal-doped catalysts with different nickel loadings; *Carbon*, **2007**, 45, 1219-1225.

[58] Ferreras, J. G. Catálisis con resinas sulfónicas de intercambio iónico en fase gaseosa: Esterificación de ácido acético con etanol. *University of Barcelona*, **1985**.

[59] Sanchez, C. L. A. Transformación de intermedios lignocelulósicos en Gamma-valerolactona: hacia un proceso catalítico eficiente. Tesis doctoral, *Universidad Rei Juan Carlos,* **2019**.

ACRONYMS

AL or α-AL: Alpha angelica lactone

CO: Carbon monoxide

DVB: Divinylbenzene

EtOH: Ethanol

FA: Formic acid

GVL: Gamma-Valerolactone

GC: Gas chromatograph

HMF: Hydroxymethylfurfural

LA: Levulinic acid

LHSV: Linear hourly space velocity

MIBK: Methyl isobutyl ketone

MTHF: 2-Methyltetrahydrofuran

RD: Dilution ratio

RT: Retention time

SOPs: Standard operating procedures

SP: Set point

VA: Valeric acid

Y_{GVL}: GVL yield

APPENDICES

APPENDIX 1: GAS CHROMATOGRAPH CALIBRATION

For GC calibration, 14 different calibration vials have been prepared. Table 14 shows the composition for every calibration vial.

Table 14: Calibration data

	% MASS				
VIAL	**LA**	**H_2O**	**GVL**	**α-AL**	**VA**
1	34.86	20.07	4.94	20.44	19.69
2	44.72	30.21	10.06	5.15	9.86
3	10.34	49.82	24.97	9.86	5.01
4	19.77	9.88	70.35	0.00	0.00
5	54.79	33.72	0.00	8.41	3.08
6	5.20	64.38	15.09	3.23	12.10
7	64.86	8.07	16.65	2.40	2.40
8	79.58	2.82	1.31	1.31	14.99
9	7.98	83.99	2.02	3.91	2.09
10	14.81	33.42	29.77	10.45	11.55
11	18.23	17.76	44.91	13.16	5.95
12	13.41	17.89	53.41	15.28	0.00
13	16.25	69.92	13.82	0.00	0.00
14	9.63	0.00	60.83	13.00	16.54

It is necessary to mention that the 6th vial has not been conclusive as the results are far from the trend of all the other experiments. In all the following explanations the results of this vial are not going to be used. The calibration of each substance has been done separately. The results obtained for Levulinic Acid are attached bellow.

Table 15: Calibration data for LA

VIAL	% MASS	AREA 1	AREA 2	AREA 3	AVERAGE	ε absolute
1	34.86	26.85	32.59	33.64	31.02	2.79
2	44.72	39.81	39.27	43.81	40.96	1.90
3	10.34	8.22	8.97	7.23	8.14	0.61
4	19.77	16.45	16.65	17.37	16.83	0.36
5	54.79	44.36	50.64	48.20	47.73	2.25
7	64.86	60.17	60.29	62.97	61.14	1.22
8	79.58	77.01	77.36	77.57	77.31	0.20
9	7.98	6.62	6.04	5.34	6.00	0.44
10	14.81	11.61	12.19	13.54	12.45	0.73
11	18.23	16.32	16.80	16.80	16.64	0.21
12	13.41	12.71	11.87	12.37	12.32	0.30
13	16.25	12.72	13.15	12.23	12.70	0.31
14	9.63	8.51	8.86	8.67	8.68	0.12

The results have been adjusted to a second order polynomial equation. To do that a polynomial regression was done.

Table 16: Regression data to adjust to a second order polynomial equation for LA

% MASS	% AREA	% AREA^2
34.86	31.02	962.53
44.72	40.96	1677.86
10.34	8.14	66.28
19.77	16.83	283.14
54.79	47.73	2278.41
64.86	61.14	3738.34
79.58	77.31	5976.89
7.98	6.00	36.04
14.81	12.45	154.94
18.23	16.64	276.81
13.41	12.32	151.66
16.25	12.70	161.25
9.63	8.68	75.35

Using the regression tool from Excel the values and their errors were able to be specified. The adjust to a second order polynomial equation for Levulinic Acid in this reaction is mentioned below.

Table 17: Polynomial calibration equation for LA

Polynomial equation	R^2
$y = (1.209 \pm 0.027)\cdot x - (0.0023 \pm 0.0004)\cdot x^2$	0.999

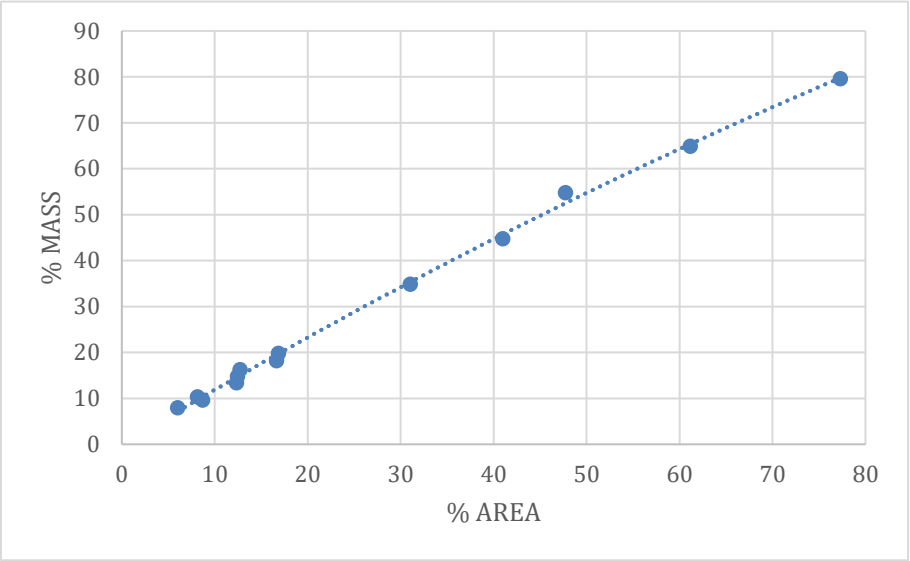

Graphic 1: Polynomial fit for calibration data of LA

The *y* value in the polynomial equation represents % in mass and the *x* value represents the area below the peak.

The same procedure has been done for the other five components. Note that in the case of the α-AL and the GVL the data points were adjusted to a linear equation.

All data tables and calibration equation can be seen below.

Table 18: Calibration data for water

VIAL	% MASS	AREA 1	AREA 2	AREA 3	AVERAGE	ε absolute
1	20.07	30.28	25.66	25.95	27.29	1.99
2	30.21	37.17	37.73	32.88	35.93	2.03
3	49.82	57.37	54.05	58.90	56.77	1.81
4	9.88	14.38	13.11	17.37	14.95	1.61
5	33.72	46.59	40.35	48.20	45.05	3.13
7	8.07	13.55	13.71	10.63	12.63	1.33
8	2.82	5.25	5.03	5.11	5.13	0.08
9	83.99	87.27	88.16	88.96	88.13	0.57
10	33.42	41.11	40.96	39.06	40.38	0.88
11	17.76	24.33	23.34	22.96	23.54	0.52
12	17.89	21.19	23.90	22.78	22.62	0.96
13	69.92	75.33	74.92	76.27	75.51	0.51
14	0.00	0.00	0.00	0.00	0.00	0.00

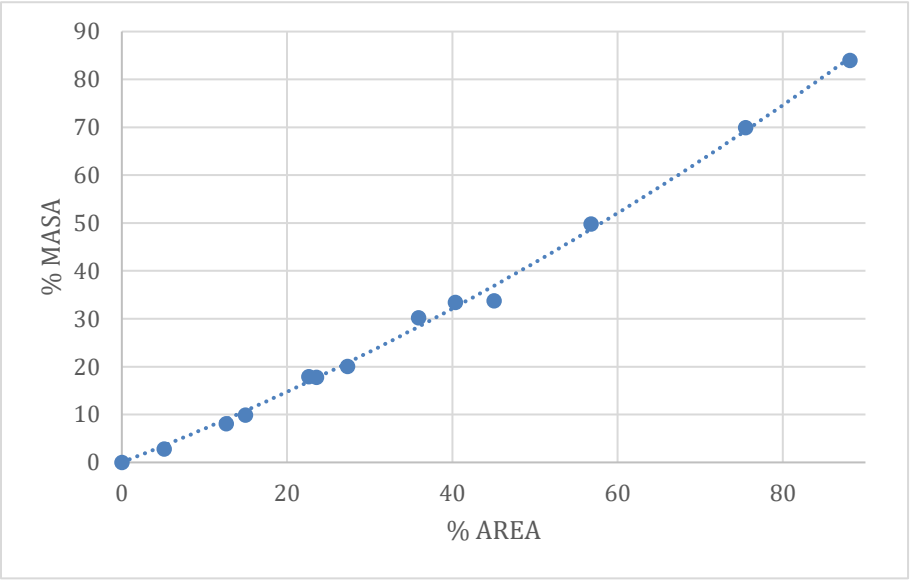

Graphic 2: Polynomial fit for calibration data of water

Table 19: Polynomial calibration equation for water

Polynomial equation	R^2
$y = (0.673 \pm 0.027) \cdot x + (0.0032 \pm 0.0004) \cdot x^2$	0.999

Table 20: Calibration data for GVL

VIAL	% MASS	AREA 1	AREA 2	AREA 3	AVERAGE	ε absolute
1	4.94	4.89	4.97	4.89	4.92	0.03
2	10.06	9.76	9.81	10.19	9.92	0.18
3	24.97	23.32	24.79	22.07	23.39	0.93
4	70.35	69.20	70.24	68.74	69.39	0.56
5	0.00	0.00	0.00	0.00	0.00	0.00
7	16.65	16.90	16.95	16.80	16.88	0.06
8	1.31	1.43	1.40	1.00	1.28	0.18
9	2.02	2.00	1.85	1.94	1.93	0.05
10	29.77	28.53	28.44	28.70	28.55	0.10
11	44.91	43.39	44.02	44.10	43.84	0.30
12	53.41	53.29	51.41	52.06	52.25	0.69
13	13.82	11.96	11.92	11.50	11.79	0.20
14	60.83	63.34	63.21	63.46	63.34	0.09

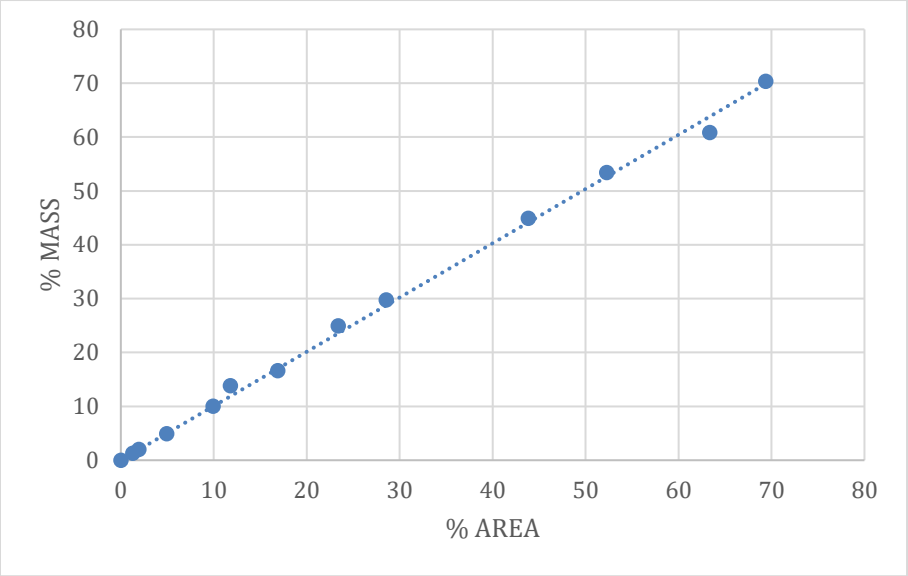

Graphic 3: Lineal fit for calibration data of GVL

Table 21: Lineal calibration equation for GVL

Lineal equation	R^2
y = (1.007 ± 0.0096)·x	0.999

Table 22: Calibration data for α-AL

VIAL	% MASS	AREA 1	AREA 2	AREA 3	AVERAGE	ε absolute
1	20.44	19.27	18.48	17.84	18.53	0.50
2	5.15	4.41	4.51	4.22	4.38	0.11
3	9.86	7.81	8.31	8.18	8.10	0.20
4	0.00	0.00	0.00	0.00	0.00	0.00
5	8.41	6.87	6.85	6.66	6.79	0.09
7	2.40	2.06	1.82	2.05	1.98	0.11
8	1.31	1.07	1.07	1.41	1.18	0.15
9	3.91	2.58	2.62	2.61	2.60	0.01
10	10.45	8.74	8.50	8.34	8.53	0.15
11	13.16	11.05	11.03	11.18	11.09	0.06
12	15.28	12.82	12.82	12.80	12.81	0.01
13	0.00	0.00	0.00	0.00	0.00	0.00
14	13.00	11.80	11.73	11.87	11.80	0.05

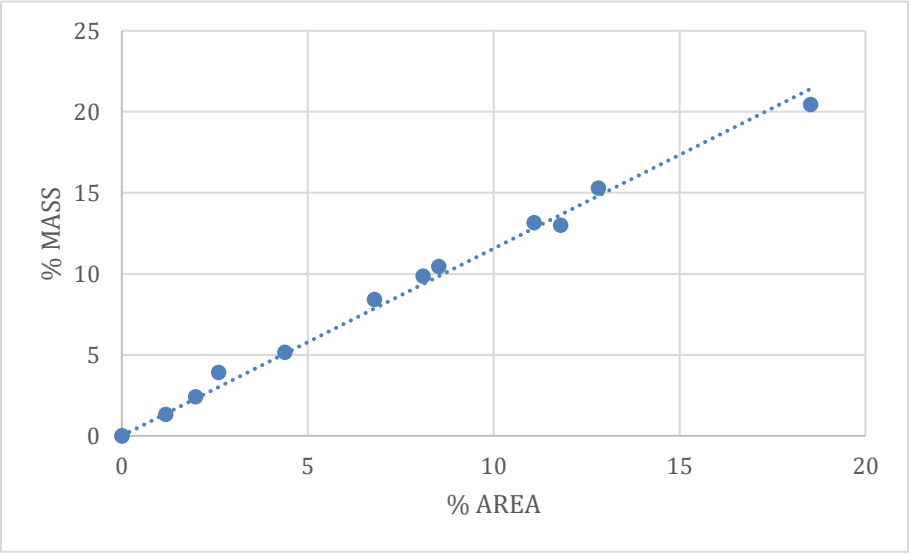

Graphic 4: Lineal fit for calibration data of α-AL

Table 23: Lineal calibration equation for α-AL

Lineal equation	R^2
$y = (1.156 \pm 0.017) \cdot x$	0.997

Table 24: Calibration data for VA

VIAL	% MASS	AREA 1	AREA 2	AREA 3	AVERAGE	ε absolute
1	19.69	18.36	18.31	18.69	18.45	0.16
2	9.86	8.85	8.69	8.91	8.81	0.09
3	5.01	3.28	3.88	3.62	3.59	0.21
4	0.00	0.00	0.00	0.00	0.00	0.00
5	3.08	2.18	2.16	2.34	2.23	0.08
7	8.03	7.32	7.23	7.57	7.37	0.13
8	14.99	14.80	14.89	14.65	14.78	0.09
9	2.09	1.53	1.34	1.31	1.39	0.09
10	11.55	10.01	10.02	10.36	10.13	0.15
11	5.95	4.92	4.84	4.96	4.90	0.05
12	0.00	0.00	0.00	0.00	0.00	0.00
13	0.00	0.00	0.00	0.00	0.00	0.00
14	16.54	16.35	16.21	16.00	16.19	0.13

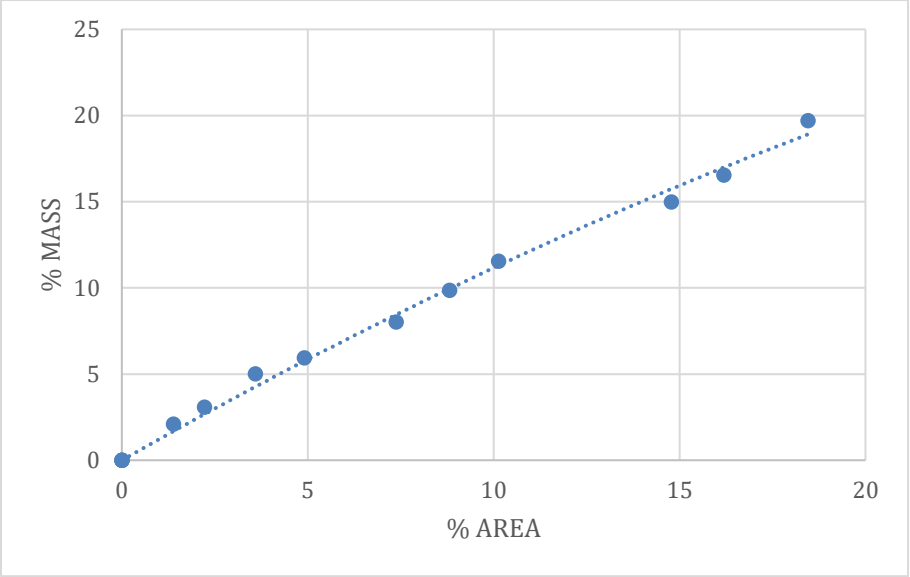

Graphic 5: Polynomial fit of calibration data for VA

Table 25: Polynomial calibration equation for VA

Polynomial equation	R^2
$y = (1.25 \pm 0.057)\cdot x - (0.0123 \pm 0.0037)\cdot x^2$	0.998

APPENDIX 2: MICROACTIVITY-REFERENCE REACTOR PID

In the following pages are attached the PID diagrams for the installation used in the present project.

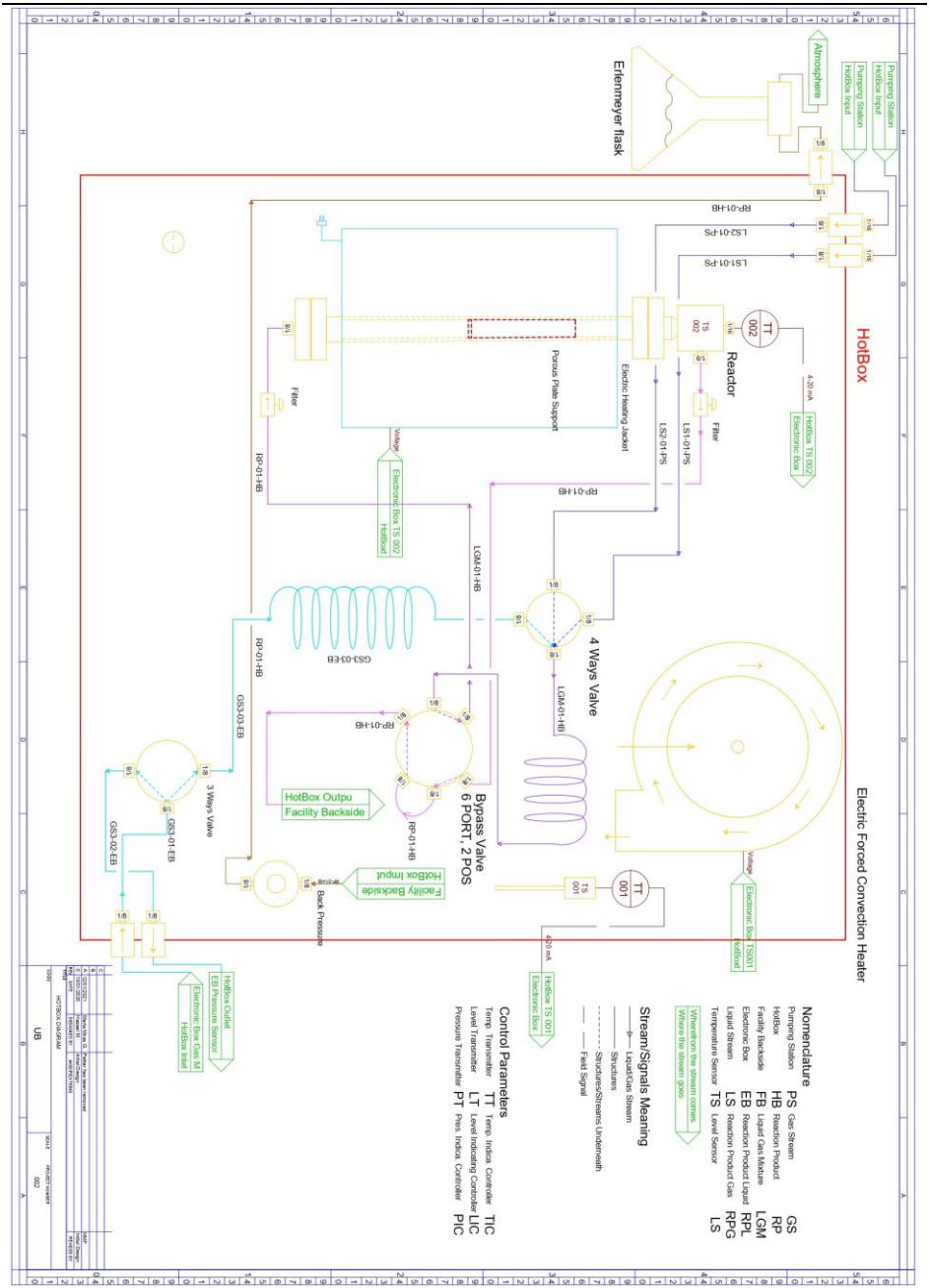

Figure 20: Hot box PID

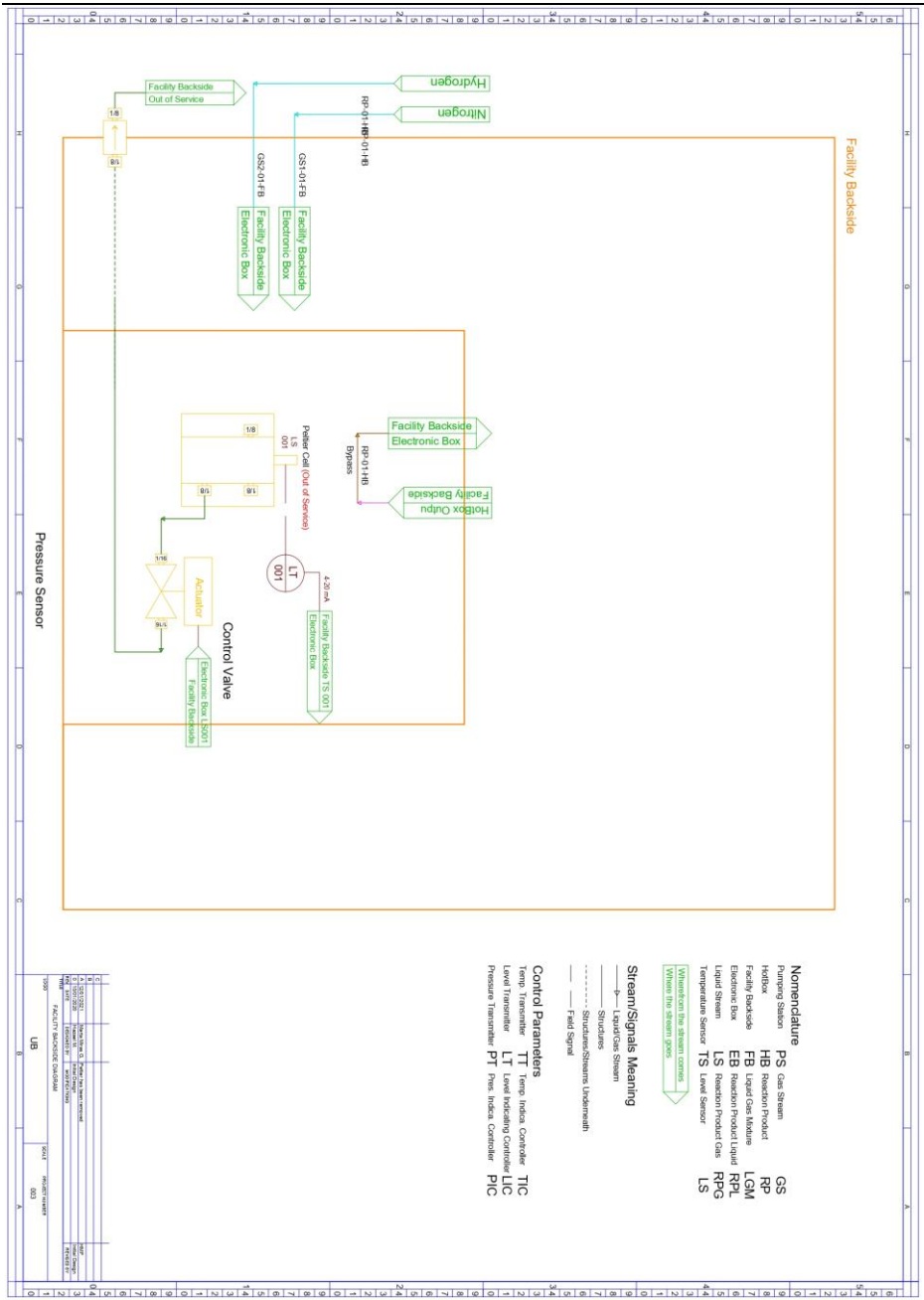

Figure 21: Facility backside PID

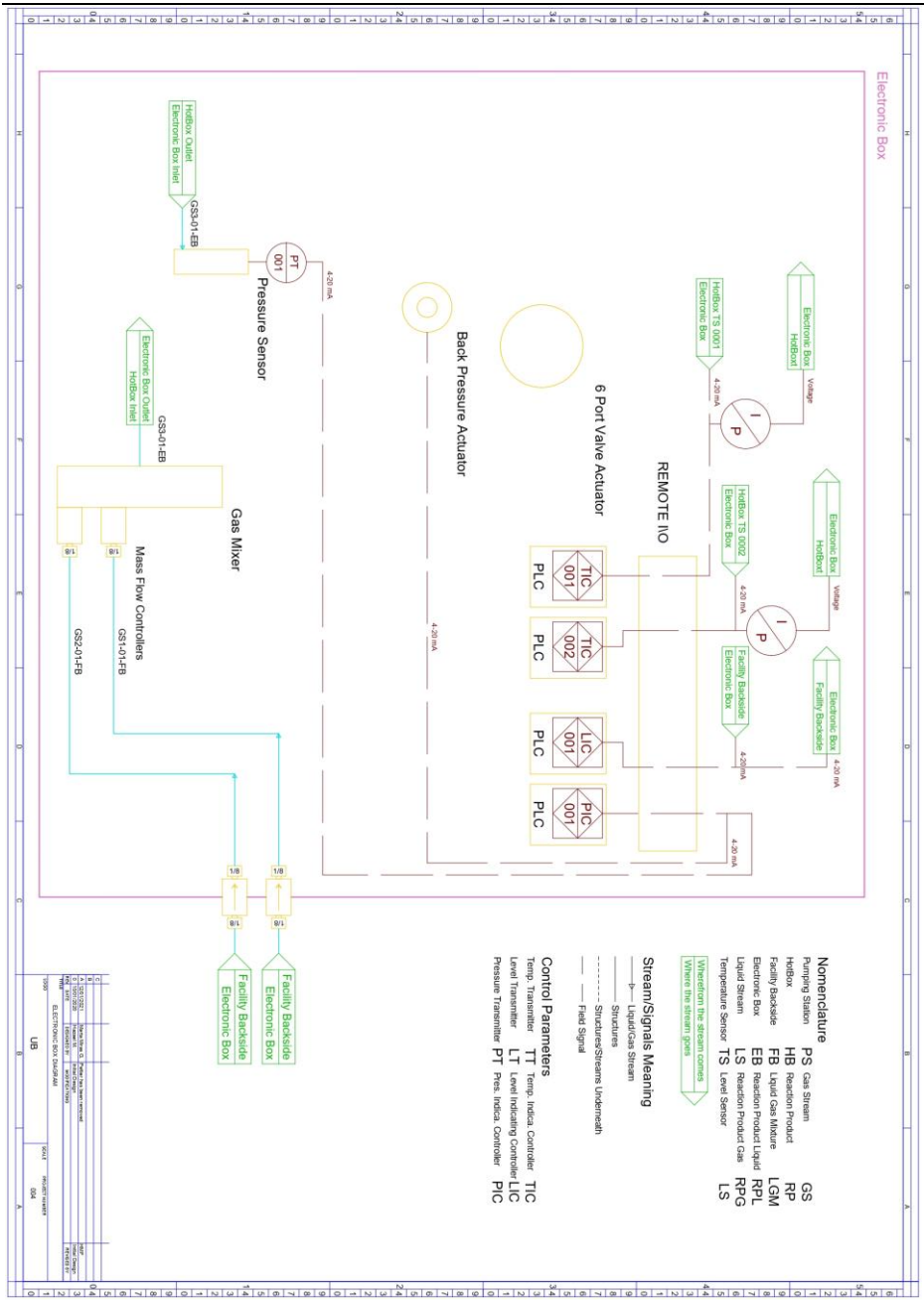

Figure 22: Electronic system PID

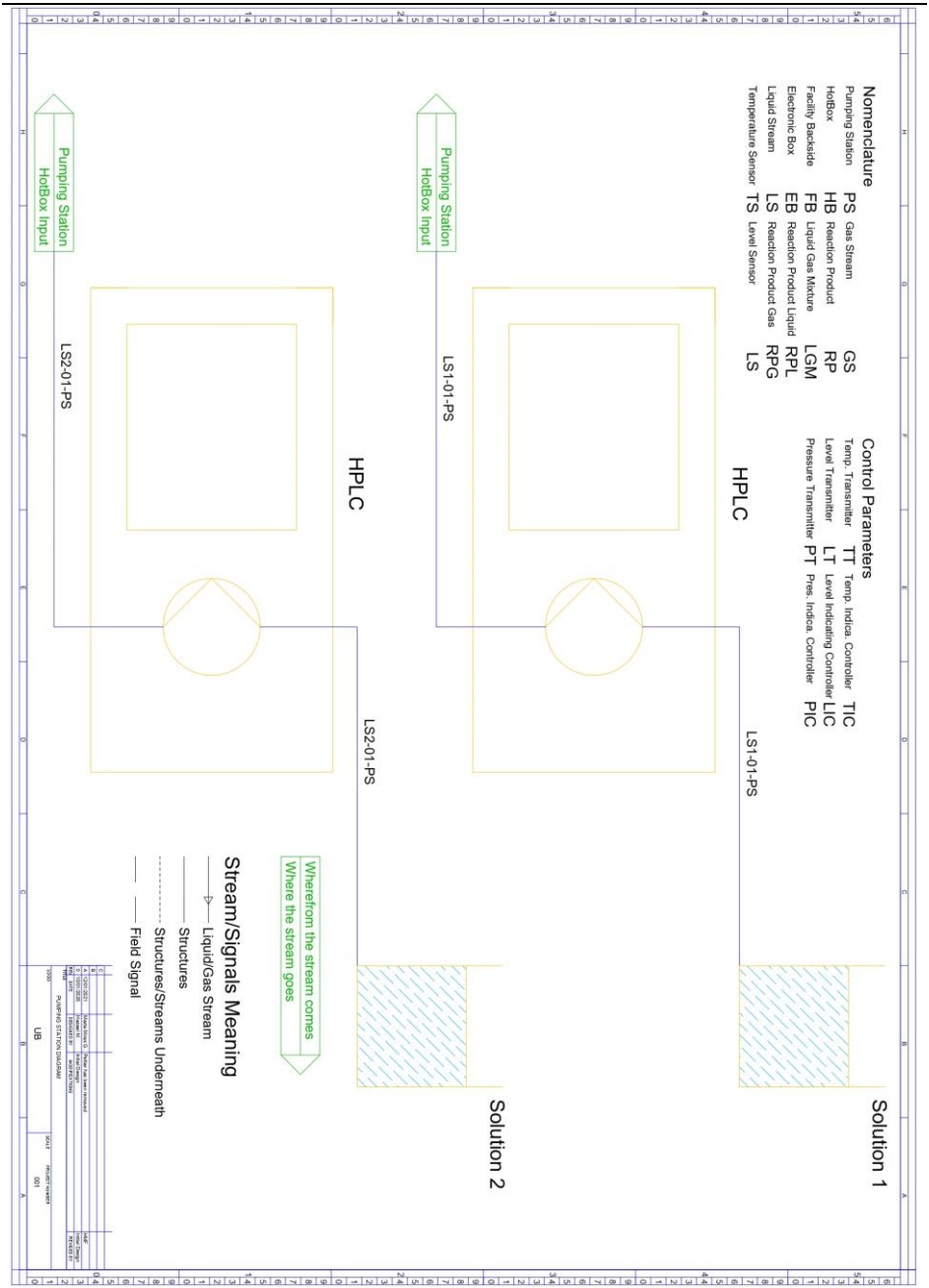

Figure 23: Pumping station PID

APPENDIX 3: GENERAL CALCULATIONS

Water and LA weights needed to prepare 1000g of 50% wt. feed solution.

$$1000\ g\ sol.\ \cdot \frac{0.5\ g\ pure\ LA}{1\ g\ sol.} \cdot \frac{1\ g\ LA\ 98\%}{0.98\ g\ pure\ LA} = 510.204\ g\ LA\ 98\%$$

$$1000 - 510.204 = 489.796\ g\ H_2O$$

Water required to solvate all functional groups of 0.5 g of catalyst.

$$0.5\ g\ cat \cdot \frac{4.8 \cdot 10^{-3}\ H^+}{1\ g\ cat} \cdot \frac{2\ mol\ H_2O}{1\ H^+} \cdot \frac{18\ g\ H_2O}{1\ mol\ H_2O} \cdot \frac{1\ mL\ H_2O}{1\ g\ H_2O} = 0.09\ mL\ H_2O$$

The meq/g cat data has been obtained from Amberlyst CH28 safety data sheet. Molecular weight of water has been extracted from water safety data sheet.

From stoichiometric information it is known that two moles of water solvate one mole of SO_3-H^+.

Volume of wet catalyst equivalent to 0.5 grams of dry catalyst.

$$0.5\ g\ dry\ cat * \frac{7.5\ mL\ wet\ cat}{2.74\ g\ dry\ cat} = 1.537\ mL\ wet\ cat$$

From previous projects [49. 50] wet and dry volume relation for Amberlyst CH28 is known.

Feed flow rate for the activity test setting a LHSV value of 4.

$$4\ \frac{mL\ feed}{mL\ wet\ cat * h} * 1.537\ mL\ wet\ cat = 6.148\ \frac{mL\ feed}{h} = 0.1025\ \frac{mL\ feed}{min}$$

Conversion from flow rate to molar rate of Nicol and Du Toit [29] hydrogen and feed flows.

To convert hydrogen flow from normal to mass flow indicator conditions. it is assumed that hydrogen follows the ideal gases equation. For normal conditions. 0 °C and 1 atm have been assumed.

$$\frac{PV}{T} = \frac{P_2V_2}{T_2} \rightarrow \frac{1\ atm * 330\ NmL/min}{273.15\ K} = \frac{30\ atm * X}{(273.15+25)K}$$
$$X = 12.007\ mL/\min H_2$$

Hydrogen flow density at mass flow indicator conditions is then:

$$\rho = \frac{P * M}{R * T} = \frac{30\ atm *..016\frac{g}{mol}}{0.821\frac{atm * L}{mol * K} * (273.15+25)K} * \frac{1\ L}{1000\ mL} = 2.47 * 10^{-4}\ \frac{g}{mL}$$

Molar flow rate conversion for Nicol and Du Toit hydrogen flow:

$$330\ \frac{mL}{min} * \frac{2.47 * 10^{-4} g}{1\ mL} * \frac{1\ mol}{2.016\ g} = 0.041\ mol/min\ H_2$$

Molar flow conversion for 3.3 mL/min flow rate of acetone:

$$\rho = 656.88\ \frac{kg}{m^3} \rightarrow 0.657\ \frac{g}{mL}$$
$$3.3\ \frac{mL}{min} * \frac{0.657\ g\ acetone}{1\ mL} * \frac{1\ mol}{58.08\ g} = 3.73 * 10^{-2}\ mol/min$$

$$Molar\ ratio = \frac{0.041\frac{mol}{\min H_2}}{3.73 * 10^{-2}\frac{mol}{\min acetone}} = 1.1$$

Hydrogen feed flow calculation for activity test SOPs to fit a 1.1 molar ratio.

To convert 50% wt. LA solution feed flow to LA molar flow. an approximate average density of the solution has been assumed.

$$0.1025\frac{mL\ feed}{min} * \frac{1.03\ g\ feed\ solution}{1mL\ feed} * \frac{0.5g\ LA}{1\ g\ solution} * \frac{1\ mol\ LA}{116.11\ g\ LA}$$
$$= 4.55 * 10^{-4}\ mol/\min LA$$

$$1.1 = \frac{x}{4.55 * 10^{-4}\frac{mol}{\min LA}} \rightarrow x = 5 * 10^{-4}\frac{mol}{\min H_2} = 4.1\ \frac{mL}{\min H_2}$$

Hydrogen solubility in water.

The following equation for hydrogen solubility in water calculation have been taken from page 1317 (8-86) of the CRC handbook of chemistry and physics [56].

$$ln(X_1) = A + \frac{B}{T*} + C * ln(T*)$$

Equation constants:

$$A = -48.1611$$

$$B = 55.2845$$

$$C = 16.8893$$

$$T* = \frac{T\ [K]}{100}$$

Where X_1 refers to the solubility in mol H_2/total mol units. All values refer to a partial pressure of the gas of 1 atm.

The solubility of hydrogen in water does not only depend on temperature. but it is also affected by the partial pressure of the gas. According to Henry's Law. the solubility of a gas in a liquid at a certain temperature is proportional to the partial pressure of the gas above the liquid:

$$X_1 = k * P_A$$

Where P_A is the partial pressure and k is a constant characteristic of the solute. the solvent and the temperature.

From CRC handbook data at 1 atm and a temperature of 130 °C the solubility of the hydrogen in water at these properties can be calculated.

$$T* = \frac{273.15 + 130}{100} = 4.03$$

$$ln(X_1) = (-48.1611) + \frac{55.2845}{4.03} + 16.8893 * ln(4.03) \rightarrow X_1$$

$$= 1.84 * 10^{-5} \frac{mol\ H_2}{total\ mol}$$

Then. the constant k of Henry's Law at 130 °C and 1 atm can be calculated.

$$1.84 * 10^{-5} = k * 1 \rightarrow k = 1.84 * 10^{-5}$$

For this system. as the only gas present is hydrogen. its partial pressure is equal to the total pressure of the system (which is 30 bar).

$$X_1 = 1.84 * 10^{-5} * 30 \rightarrow X_1 = 5.52 * 10^{-4} \frac{mol\ H_2}{total\ mol}$$

Relation between the dry weight of the catalyst and its dry and wet volume.

Relation obtained from Gutierrez [49] and Martínez [50] previous projects.

Table 26: Weight and volume relation for Amberlyst CH28

	Dry	Wet
Weight [g]	2.74	5.42
Volume [mL]	3.5	7.5
Density [g/mL]	0.78	0.72

Minimum hydrogen needed to reduce all the palladium present in the catalyst used.

The reaction mechanism for the palladium reduction:

$Pd^{2+} + 2\ e^- \rightarrow Pd^0$

$H_2 \rightarrow 2\ H^+ + 2\ e^-$

Assuming 0.5 grams of catalyst used. From catalyst data sheet it is known that it has 0.7% minimum of palladium in dry basis.

$$0.5\ g\ cat * \frac{0.7\ g\ Pd^{2+}}{100\ g\ cat} * \frac{1\ mol\ Pd}{106.4\ g} = 3.29 * 10^{-5}\ mol\ Pd^{2+}$$

$$3.29 * 10^{-5}\ mol\ Pd^{2+} * \frac{1\ mol\ H_2}{1\ mol\ Pd^{2+}} = 3.29 * 10^{-5}\ mol\ H_2$$

It has considered hydrogen as an ideal gas.

$$PV = nRT \rightarrow V = \frac{nRT}{P}$$

At experiment conditions:

$$V = \frac{3.29 * 10^{-5} * 0.082 * (90 + 273.15)}{30} = 0.032\ mL\ H_2$$